Docosahexaenoic acid lowers cardiac mitochondrial enzyme activity by replacing linoleic acid in the phospholipidome

E. Madison Sullivan[‡§1], Edward Ross Pennington[‡§¶1], Genevieve C. Sparagna[‖], Maria J. Torres[§], P. Darrell Neufer[§**], Mitchel Harris[‡], James Washington[‡§], Ethan J. Anderson[‡‡], Tonya N. Zeczycki[‡§], David A. Brown[§§], and Saame Raza Shaikh[‡§¶2]

From the [‡]Department of Biochemistry and Molecular Biology, [§]East Carolina Diabetes and Obesity Institute, and [**]Department of Physiology, Brody School of Medicine, East Carolina University, Greenville, North Carolina 27834, the [¶]Department of Nutrition, Gillings School of Global Public Health and School of Medicine, University of North Carolina at Chapel Hill, Chapel Hill, North Carolina 27599, the [‖]Department of Medicine, Division of Cardiology, University of Colorado Denver Anschutz Medical Campus, Aurora, Colorado 80045, the [‡‡]Department of Pharmaceutical Sciences and Experimental Therapeutics, College of Pharmacy, Fraternal Order of Eagles Diabetes Research Center, University of Iowa, Iowa City, Iowa 52242, and the [§§]Department of Human Nutrition, Foods, and Exercise, Virginia Tech Corporate Research Center, Blacksburg, Virginia 24060

Edited by George M. Carman

Cardiac mitochondrial phospholipid acyl chains regulate respiratory enzymatic activity. In several diseases, the rodent cardiac phospholipidome is extensively rearranged; however, whether specific acyl chains impair respiratory enzyme function is unknown. One unique remodeling event in the myocardium of obese and diabetic rodents is an increase in docosahexaenoic acid (DHA) levels. Here, we first confirmed that cardiac DHA levels are elevated in diabetic humans relative to controls. We then used dietary supplementation of a Western diet with DHA as a tool to promote cardiac acyl chain remodeling and to study its influence on respiratory enzyme function. DHA extensively remodeled the acyl chains of cardiolipin (CL), monolyso-CL, phosphatidylcholine, and phosphatidylethanolamine. Moreover, DHA lowered enzyme activities of respiratory complexes I, IV, V, and I + III. Mechanistically, the reduction in enzymatic activities was not driven by a dramatic reduction in the abundance of supercomplexes. Instead, replacement of tetralinoleoyl-CL with tetradocosahexaenoyl-CL in biomimetic membranes prevented formation of phospholipid domains that regulate enzyme activity. Tetradocosahexaenoyl-CL inhibited domain organization due to favorable Gibbs free energy of phospholipid mixing. Furthermore, *in vitro* substitution of tetralinoleoyl-CL with tetradocosahexaenoyl-CL blocked complex IV binding. Finally, reintroduction of linoleic acid, via fusion of phospholipid vesicles to mitochondria isolated from DHA-fed mice, rescued the major losses in the mitochondrial phospholipidome and complexes I, IV, and V activities. Altogether, our results show that replacing linoleic acid with DHA lowers select cardiac enzyme activities by potentially targeting domain organization and phospholipid–protein binding, which has implications for the ongoing debate about polyunsaturated fatty acids and cardiac health.

Mitochondria have a central role in cardiac physiology by handling differing substrates such as pyruvate and fatty acids to produce the ATP needed to maintain homeostasis. In a range of metabolic diseases such as obesity, type 2 diabetes, heart failure, ischemia–reperfusion injury, and diabetic cardiomyopathies, cardiac mitochondria are subject to considerable dysregulation (1–5). One key impairment with cardiac mitochondria is the extensive remodeling of phospholipid acyl chains, most notably of the unique mitochondrion-specific phospholipid, cardiolipin (CL)[3] (6, 7). For example, in diabetic cardiomyopathies, CL acyl chains undergo modifications that broadly include the depletion of the most abundant CL species $(18:2)_4$, as well as an increase in longer polyunsaturated acyl chains (8, 9). In fact, the remodeling of mitochondrial phospholipid acyl chains is not just limited to cardiomyopathies, but is also reported with various other conditions such as aging, obesity, and Barth syndrome (10, 11).

The mechanisms by which phospholipid acyl chain remodeling promotes mitochondrial dysfunction remain unclear. Phospholipid acyl chains, particularly linoleic acid associated with CL, bind a multitude of trans-membrane and membrane-associated enzymes to regulate their activity. For instance, CL binds oxidative phosphorylation complexes I and III–V and the mobile electron carrier cytochrome *c* (12–17). However, it is unknown how remodeling of CL to specific fatty acids influences enzyme function.

[3] The abbreviations used are: CL, cardiolipin; $(18:2)_4$CL, tetralinoleoyl-cardiolipin; $(22:6)_4$CL, tetradocosahexaenoyl-cardiolipin; DHA, docosahexaenoic acid; EPA, eicosapentaenoic acid; MLCL, monolyso-cardiolipin; PC, phosphatidylcholine; PE, phosphatidylethanolamine; LUV, large unilamellar vesicle; GUV, giant unilamellar vesicle; BisTris, 2-[bis(2-hydroxyethyl)amino]-2-(hydroxymethyl)propane-1,3-diol; PS, phosphatidylserine; PI, phosphatidylinositol; Chol, cholesterol; SPR, surface plasmon resonance; NAO, nonyl acridine orange; MLV, multilamellar vesicle; AUC, area under the curve; WD, Western diet; CIV, complex IV.

One unique remodeling event in the mitochondrial phospholipidome is an increase in the abundance of phospholipid species containing the long chain *n*-3 polyunsaturated fatty acid (PUFA) docosahexaenoic acid (DHA, 22:6) (6, 8, 9, 18). The elevation of cardiac DHA in differing cardiovascular diseases is highly paradoxical because this fatty acid is considered cardioprotective in animal models with some supporting evidence in humans (19, 20). A recent systematic review on the effects of *n*-3 PUFA supplementation in human subjects suggested that long-chain *n*-3 PUFAs can be used for ameliorating cardiovascular disease risk factors (21). However, not all research supports the health benefits of DHA. For instance, a rodent study showed that DHA did not improve cardiomyopathy induced by a Western diet (22).

Here, we used dietary intervention as a tool to study remodeling of mitochondrial phospholipids on respiratory enzyme activity. We first confirmed that cardiac DHA levels are elevated in human diabetics. We then established the metabolic profile of mice consuming Western diets in the absence or presence of DHA in addition to eicosapentaenoic acid (EPA). Next, the effects of experimental diets on the mitochondrial phospholipidome were investigated. The focus was on phosphatidylcholine (PC), phosphatidylethanolamine (PE), and CL because they are the most abundant phospholipids in the mitochondria by mass at 40, 30, and 15–20%, respectively (23). We then determined whether the experimental diets impaired mitochondrial respiratory enzyme activities because CL binds several of these enzymes (14, 16, 24–29). Mechanistically, we investigated whether DHA lowered enzyme activities due to modifications in the formation of supercomplexes, assembly of lipid domains that regulate protein activity, and phospholipid–protein-binding interactions (30–32). Finally, experiments were conducted to determine whether reintroduction of linoleic acid into mitochondria isolated from mice consuming DHA rescued remodeling in the phospholipidome and thereby enzymatic function.

Results

Cardiac DHA levels are elevated in human diabetics

Data from rodent studies demonstrate that cardiac DHA levels are elevated in different diseases (9, 18); however, evidence in humans in lacking. Therefore, cardiac DHA levels from non-diabetic and diabetic subjects were first assayed. Mitochondria could not be isolated because there was extremely limited tissue samples from surgery. Furthermore, fatty acid analyses had to be conducted with total extracted fatty acids due to the small amount of tissue obtained during surgery. Analyses with gas chromatography revealed that diabetics, compared to non-diabetic controls, had no changes in the relative levels of saturated fatty acids (Fig. 1A). The monounsaturated fatty acid 16:1 was lowered by 2.4-fold with diabetic subjects relative to the non-diabetics (Fig. 1B). *n*-6 PUFA levels were not modified (Fig. 1C). Analyses of the major *n*-3 PUFAs showed that DHA levels were increased by 1.7-fold for the diabetic subjects compared with non-diabetic controls (Fig. 1D).

Subsequent studies were conducted with mice. It was first established how murine experimental diets influenced fat/lean mass, glucose clearance, and fasting insulin levels. The effects of EPA and DHA were tested at two different time points, including consumption of the fatty acids for 14 weeks or for 4 weeks (Fig. 2A). Mice fed the Western diet and the EPA- or DHA-enriched Western diets had increased total body weights by 1.3–1.4-fold relative to the lean control (Fig. 2B). The increase in total body weight was accounted for by an increase in fat mass with the Western and EPA- or DHA-enriched Western diets by 1.9–2.1-fold relative to the control (Fig. 2C). Mice fed the Western + EPA diet (14 and 4 weeks) and the Western + DHA diet (4 weeks) had elevated lean mass compared with lean animals (Fig. 2D). Mice fed the Western diets in the absence or presence of EPA or DHA generally had diminished glucose clearance (Fig. 2E), as quantified by the area under the curve (AUC) for glucose clearance (Fig. 2F). The only exception was the Western diet + EPA (4 weeks) (Fig. 2F). Mice fed the Western diets in the absence and presence of EPA (4 weeks) or DHA (14 and 4 weeks) had increased fasting insulin levels in comparison with lean mice (Fig. 2G). The Western + DHA diet (14 and 4 weeks) increased fasting glucose levels compared with the control and/or the Western diet (for 14 weeks) (Fig. 2H). HOMA-IR scores were consistently increased with all of the Western diets, except the WD + EPA (14 weeks), relative to lean mice (Fig. 2I). There were no statistically significant differences between EPA and DHA (14 and 4 weeks) for HOMA-IR scores. Altogether, the data suggested that supplementation with EPA or DHA did not improve glucose clearance, although long-term intake with EPA did not increase the HOMA-IR score relative to lean mice, consistent with previous work (33).

Murine cardiac mitochondrial CL and monolyso-CL acyl chains are dramatically remodeled in response to Western diets in the absence and presence of EPA and DHA

We next established how the Western diets, particularly in the presence of EPA and DHA, targeted CL and monolyso-CL (MLCL) acyl chains. An example of the raw LC/MS data are presented in Fig. S1A–D. LC/MS analyses are presented as heat maps in Fig. 3. CL species were classified as either major (Fig. 3A), intermediate (Fig. 3B), or minor (Fig. 3C) in terms of abundance. MLCL levels are shown in Fig. 3D.

The most abundant CL species, $(18:2)_4$, was robustly reduced with all of the Western diets by 4.3–20.0-fold (Fig. 3A and Fig. S2, A–F). The Western diet, in the absence of EPA (4 and 14 weeks) or DHA (4 and 14 weeks), also increased a range of other major CL species relative to the control and the Western diet (Fig. 3A). CL species containing 22:6 were elevated in response to EPA intervention and robustly with DHA intervention (4 and 14 weeks). The increase in differing CL species came at the expense of lowering a range of CL species, notably containing 18:2 and 20:4 acyl chains (Fig. 3A). Several intermediate and minor CL species were also increased or decreased with the Western diet, in the absence or presence of EPA or DHA, when compared with the control by 2.0–14.0-fold (Fig. 3, B and C). There were also some differences between EPA and DHA (Fig. S2, A–F).

ASBMB

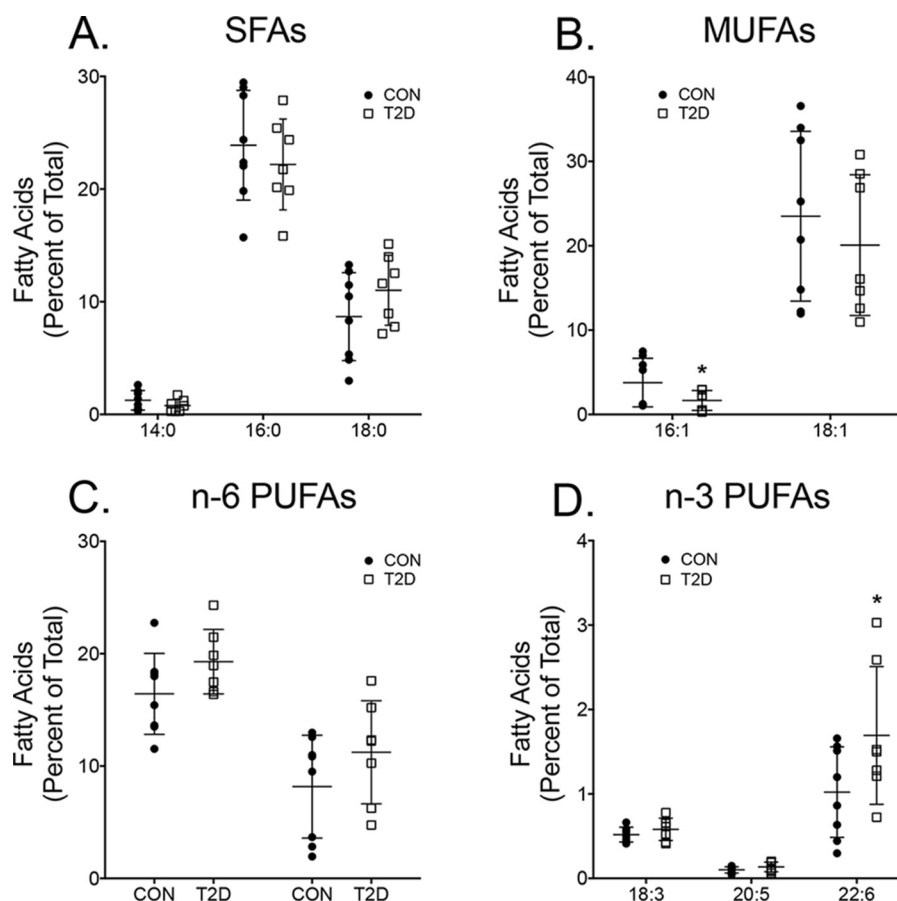*J. Biol. Chem.* (2018) 293(2) 466–483 **467**

Figure 1. Type 2 diabetic subjects have elevated cardiac DHA (22:6) levels relative to controls. Relative percentages of saturated fatty acids (*SFAs*) (*A*), monounsaturated fatty acids (*MUFAs*) (*B*), *n*-6 polyunsaturated fatty acids (*PUFAs*) (*C*), and *n*-3 PUFAs for control (*CON*) and type 2 diabetics (*T2D*) (*D*) are shown. Values represent total fatty acids that were extracted from human tissue. Data are the average ± S.D. from 7 to 8 subjects per group. *Asterisks* indicate significance from control (*, $p < 0.05$).

Murine cardiac mitochondrial PC and PE acyl chains are remodeled in response to a Western diet in the absence and presence of EPA and DHA

LC/MS analyses were also conducted with PC and PE phospholipids. Generally, the Western diet in the absence and presence of EPA (14 and 4 weeks) and DHA (14 and 4 weeks) lowered the abundance of PCs containing 16:0, 18:1, 18:2, and 20:3 acyl chains by 1–2-fold compared with the lean controls (Fig. 4A). For some species such as (18:2)$_2$PC, the effects were more robust with DHA (14 and 4 weeks) compared with EPA (14 and 4 weeks) (Fig. 4A). DHA also notably increased the levels of (18:2)(20:4)PC compared with control, Western diet, and Western diet + EPA fed mice. Similar trends were observed with PEs, where the Western diet in the absence or presence of EPA (14 and 4 weeks) and DHA (14 and 4 weeks) lowered species containing 16:0, 18:1, and 18:2 acyl chains (Fig. 4B). DHA had stronger effects than EPA on some PEs (Fig. 4B).

Cardiac mitochondrial respiratory enzyme activities are decreased with the EPA- and DHA-enriched Western diets

Subsequent experiments addressed whether the aforementioned changes in the mitochondrial phospholipidome were associated with impaired respiratory enzyme activities. We focused on long-term intake of EPA and DHA (14 weeks). Strikingly, mice that consumed the Western diet did not have a

reduction in enzyme activities and combined enzyme activities when compared with the lean control (Fig. 5, *A*–*G*). The Western + EPA and Western + DHA diets (14 weeks), respectively, reduced complex I activity by 1.8- and 1.9-fold relative to the control diet (Fig. 5A). The EPA- and DHA-containing diets had no effect on complex II (Fig. 5B) and complex III (Fig. 5C) activities. Complex IV activity was lowered with the EPA- or DHA-enriched Western diets relative to the control and/or Western diet by 1.8–2.7-fold (Fig. 5D). The Western + DHA diet (14 weeks) also modestly reduced complex V activity by 0.6-fold relative to the control (Fig. 5E). The Western + DHA diet decreased the combined activities of complex I + III by 2.0-fold compared with the control (Fig. 5F). There was no effect of EPA- and DHA-enriched Western diets on complex II + III activities (Fig. 5G).

EPA and DHA do not robustly suppress formation of the major supercomplexes

The next study addressed whether decreased enzyme-specific activities with EPA or DHA (14 weeks) were mechanistically driven by a reduction in mitochondrial supercomplex formation or in the expression levels of the complexes (34). Long-term intake of EPA or DHA had no major effect on the majority of the supercomplexes, which are depicted as supercomplexes
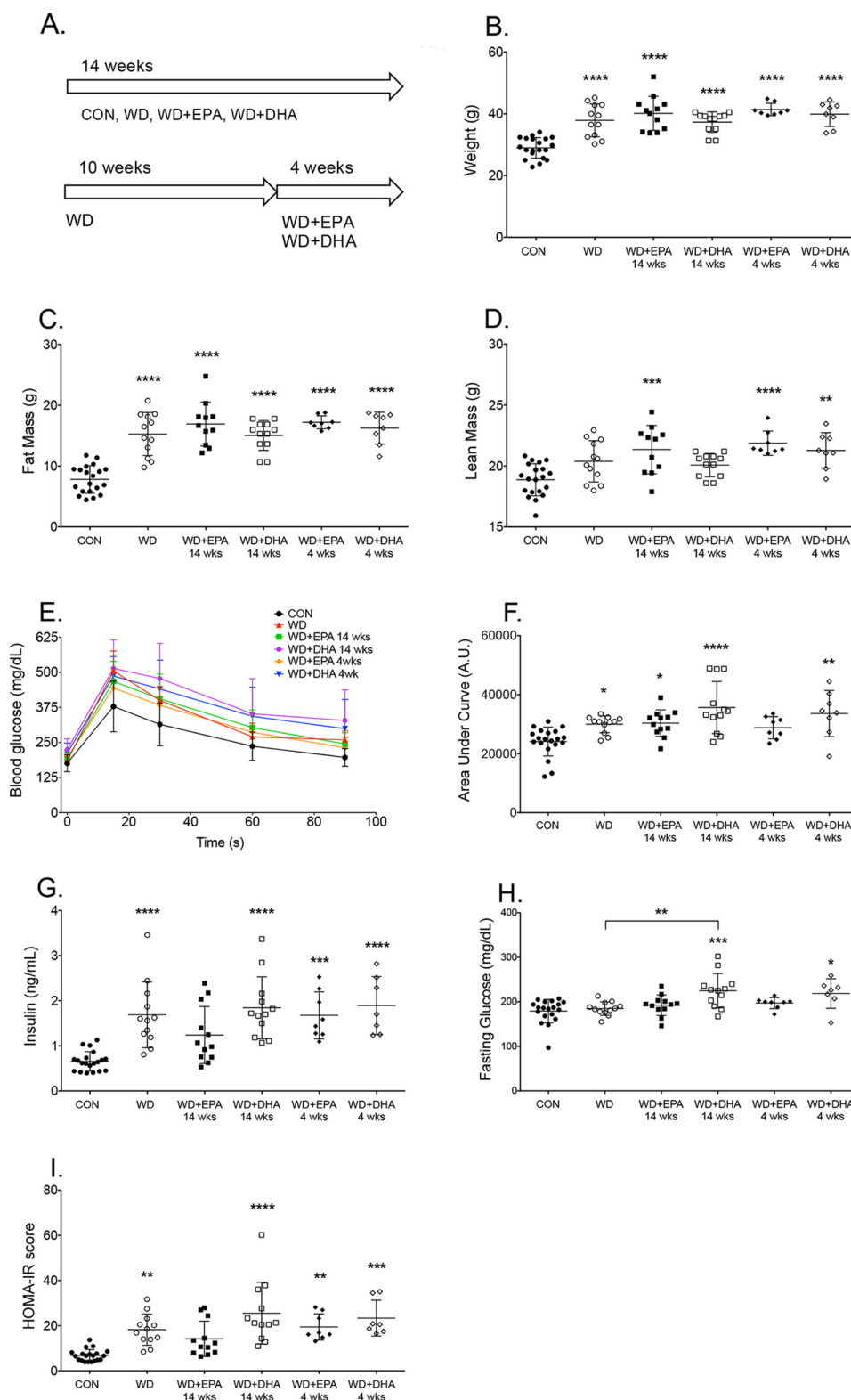
Figure 2. Metabolic profile of mice consuming a Western diet in the absence or presence of EPA and DHA for differing time points. *A,* schematic of the diet feeding schedule for mice consuming the control (*CON*), Western diet (*WD*), and Western diet containing EPA or DHA ethyl esters. *B,* body weights at the end of the 14-week feeding period. Fat (*C*) and lean (*D*) mass was determined by Echo-MRI. *E,* whole-body glucose tolerance test was performed by intraperitoneal injection of glucose after a 5-h fast. *F,* AUC, calculated by integration of the raw glucose tolerance test curves shown in *E. G,* fasting insulin; *H,* fasting glucose levels. *I,* homeostasis model assessment for insulin resistance (HOMA-IR) index scores. Data are the average $\pm$ S.D. from 8 to 20 independent experiments. *Asterisks* indicate significance from control (*CON*) (*, $p < 0.05$; **, $p < 0.01$; ***, $p < 0.001$; ****, $p < 0.0001$). *Horizontal bars* with *asterisks* indicate significance between treatments. For simplicity, statistical significance is not indicated between time points (14 and 4 weeks).
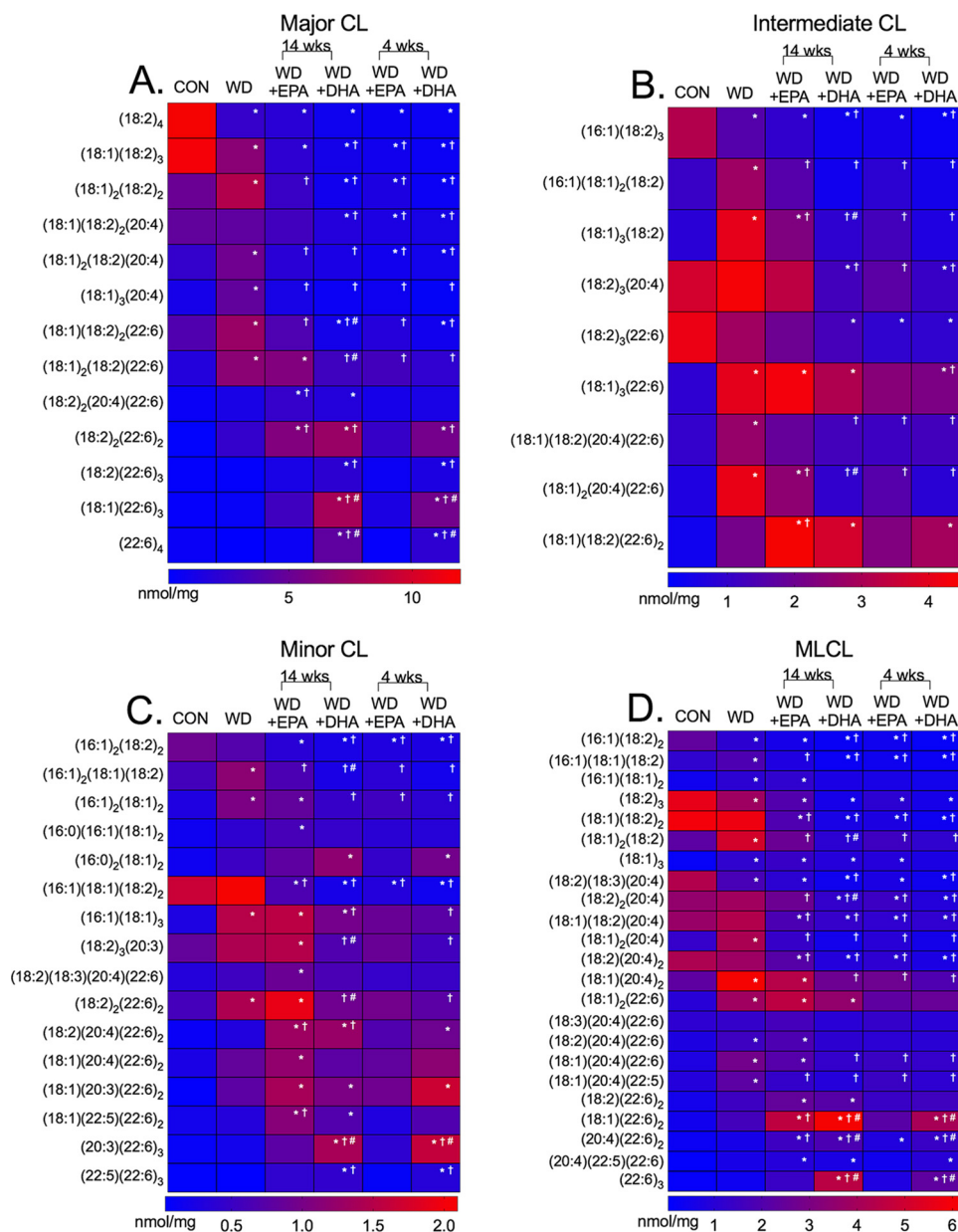
Figure 3. Cardiac mitochondrial cardiolipin acyl chains are remodeled in response to a Western diet in the absence and presence of EPA and DHA. Heat maps of major (*A*), intermediate (*B*), and minor (*C*) CL acyl chains for mice consuming a control (*CON*), Western diet (*WD*), WD + EPA, and WD + DHA are shown. *D*, monolyso-CL species in cardiac mitochondria are also shown. Data are the average from five independent experiments. *Asterisks* indicate significance from control (*, $p < 0.05$). *Daggers* indicate significance relative to the WD (†, $p < 0.05$), and *hash tags* indicate significance between EPA and DHA at 14 or 4 weeks (#, $p < 0.05$). For simplicity, statistical significance is not indicated between time points (14 and 4 weeks).

1–5 (Fig. S3, *A–F*) (35). The notable exception was that mice consuming the Western + DHA diet had a reduction in the amount of supercomplex 4 when compared with the control and Western diets by 2.5- and 2.7-fold, respectively (Fig. S3*E*). Blue native-PAGE analysis also revealed that there were no changes in the expression of complexes I–V in the Western and EPA- or DHA-enriched Western diets compared with the lean control (data not shown).

Replacement of (18:2)₄CL with (22:6)₄CL prevents the formation of lipid domains by influencing the Gibbs free energy of lipid–lipid mixing

Given that DHA did not robustly impair the abundance of the majority of supercomplexes, we investigated another

potential mechanism by which respiratory enzyme activity could be lowered with DHA. We used a biophysical approach to determine whether DHA could target the formation of CL domains, which control phospholipid–protein binding that is critical for optimal enzyme function (36). Biomimetic mitochondrial membranes modeling the composition of the cardiac inner mitochondrial membrane were used because they allow for a controlled model system. $(22:6)_4$CL was specifically investigated given that it is a symmetric phospholipid and was elevated in response to DHA in the diet (Fig. 3*A* and Fig. S2*F*). Cytochrome *c* was added to the biomimetic membranes because it known to induce domain formation in giant unilamellar vesicles (37).
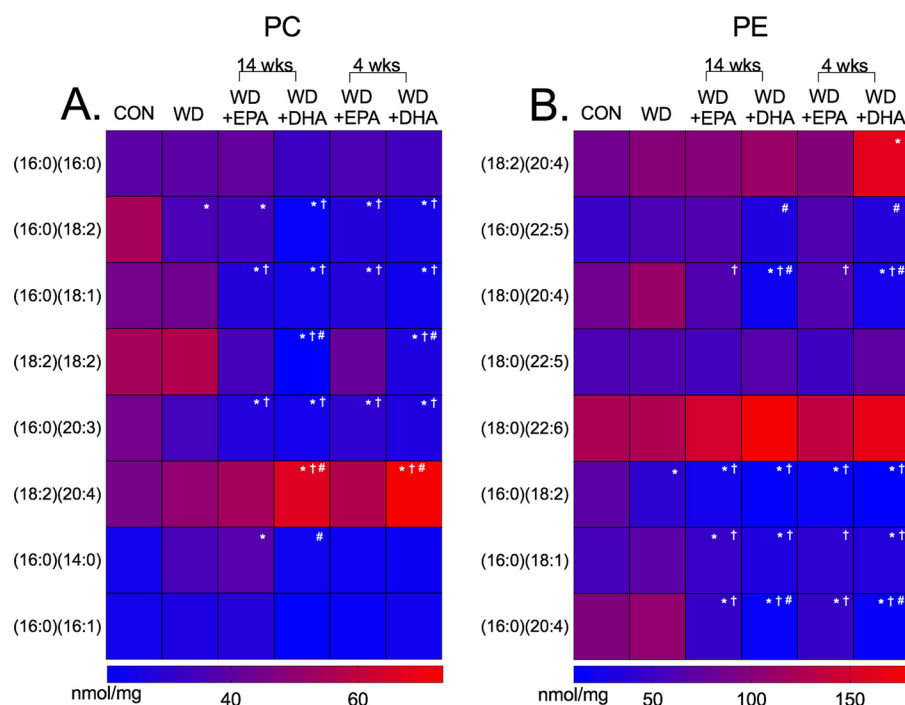
Figure 4. Cardiac mitochondrial PC and PE acyl chains are remodeled in response to a Western diet in the absence and presence of EPA and DHA. Heat maps of PC (*A*) and PE (*B*) acyl chains in cardiac mitochondria for mice consuming a control (*CON*), Western diet (*WD*), WD + EPA, and WD + DHA are shown. Data are the average from five independent experiments. *Asterisks* indicate significance from control (*, $p < 0.05$). *Daggers* indicate significance from WD (†, $p < 0.05$), and *hash tags* indicate significance between EPA and DHA at 14 or 4 weeks (#, $p < 0.05$). For simplicity, statistical significance is not indicated between time points (14 and 4 weeks).

Imaging revealed that $(18:2)_4CL$ promoted the formation of phase-separated domains (as visualized by NAO), which were diminished upon replacement of $(18:2)_4CL$ with $(22:6)_4CL$ (Fig. 6A). A range of phase-separated domain areas was measured with the NAO fluorescent probe and are presented as a frequency distribution. A Gaussian fit was applied to the frequency distributions with larger areas reflecting greater coverage of the NAO fluorophore on the perimeter of the giant unilamellar vesicles (Fig. 6B). Visual inspection of the frequency distributions of the domains were clearly different between $(18:2)_4CL$ and $(22:6)_4CL$ (Fig. 6B). Quantification of the average area occupied by the NAO probe showed that DHA prevented formation of phase-separated domains (Fig. 6C).

To explain how $(22:6)_4CL$ prevented domain formation, monolayers of the same lipid mixtures modeling the inner mitochondrial membrane were constructed containing either $(18:2)_4CL$ (Fig. 6D) or $(22:6)_4CL$ (Fig. 6E) in the absence or presence of cytochrome *c*. This model system allowed us to investigate phospholipid mixing properties that are central for the formation of phase-separated lipid domains (38). The monolayer pressure area isotherms (Fig. 6, *D and E*) were then used to calculate the change in excess area per molecule in response to cytochrome *c*. The excess area per molecule values provide a quantitative change at the angstrom level on how phospholipids are mixing or de-mixing (*i.e.* lipid–lipid miscibility) (39).

In biomimetic mitochondrial monolayers containing $(18:2)_4CL$, the change in excess area per molecule was positive, indicating unfavorable lipid mixing (*i.e.* formation of phase-separated domains) (Fig. 6F). Upon replacement of $(18:2)_4CL$ with $(22:6)_4CL$, this value became negative, indicating favorable

mixing between phospholipids (*i.e.* no formation of phase-separated domains). We further calculated the change in Gibbs free energy of mixing upon the addition of cytochrome *c*. $(18:2)_4CL$ had a positive change in Gibbs free energy of mixing, indicating unfavorable mixing of phospholipids (Fig. 6G). Replacement of $(18:2)_4CL$ with $(22:6)_4CL$ shifted the Gibbs free energy of mixing to a favorable negative value. Thus, these results established that $(18:2)_4CL$ promoted phase-separated domains due to unfavorable lipid mixing. In contrast, the lack of domains in the presence of $(22:6)_4CL$ was driven by favorable Gibbs free energy of mixing between phospholipids.

Replacement of $(18:2)_4CL$ with $(22:6)_4CL$ diminishes interactions with complex IV

CL domains are hypothesized to create a microenvironment that regulates protein activity through direct phospholipid–protein binding (12, 15, 25, 40) Thus, we further investigated whether replacement of $(18:2)_4CL$ with $(22:6)_4CL$ in biomimetic mitochondrial large unilamellar vesicles (LUVs) impaired binding interactions with immobilized complex IV using surface plasmon resonance (SPR) (41). Complex IV was selected because its activity was lowered with DHA, suggesting that the known high-affinity, CL-specific binding sites (27, 42–44) may be unable to accommodate remodeled CL. SPR binding curves showed dramatic differences in binding interactions between complex IV and LUVs containing either $(18:2)_4CL$ (Fig. 7A) or $(22:6)_4CL$ (Fig. 7B). Strikingly, there was a lack of detectable LUV–CIV interactions in the presence of $(22:6)_4CL$ at LUV concentrations nearly 100-fold higher than the reported apparent K_d value for CL binding to the high- and low-affinity sites on CIV (<0.1 and $4\ \mu M$, respectively) (43). Fitting of the binding
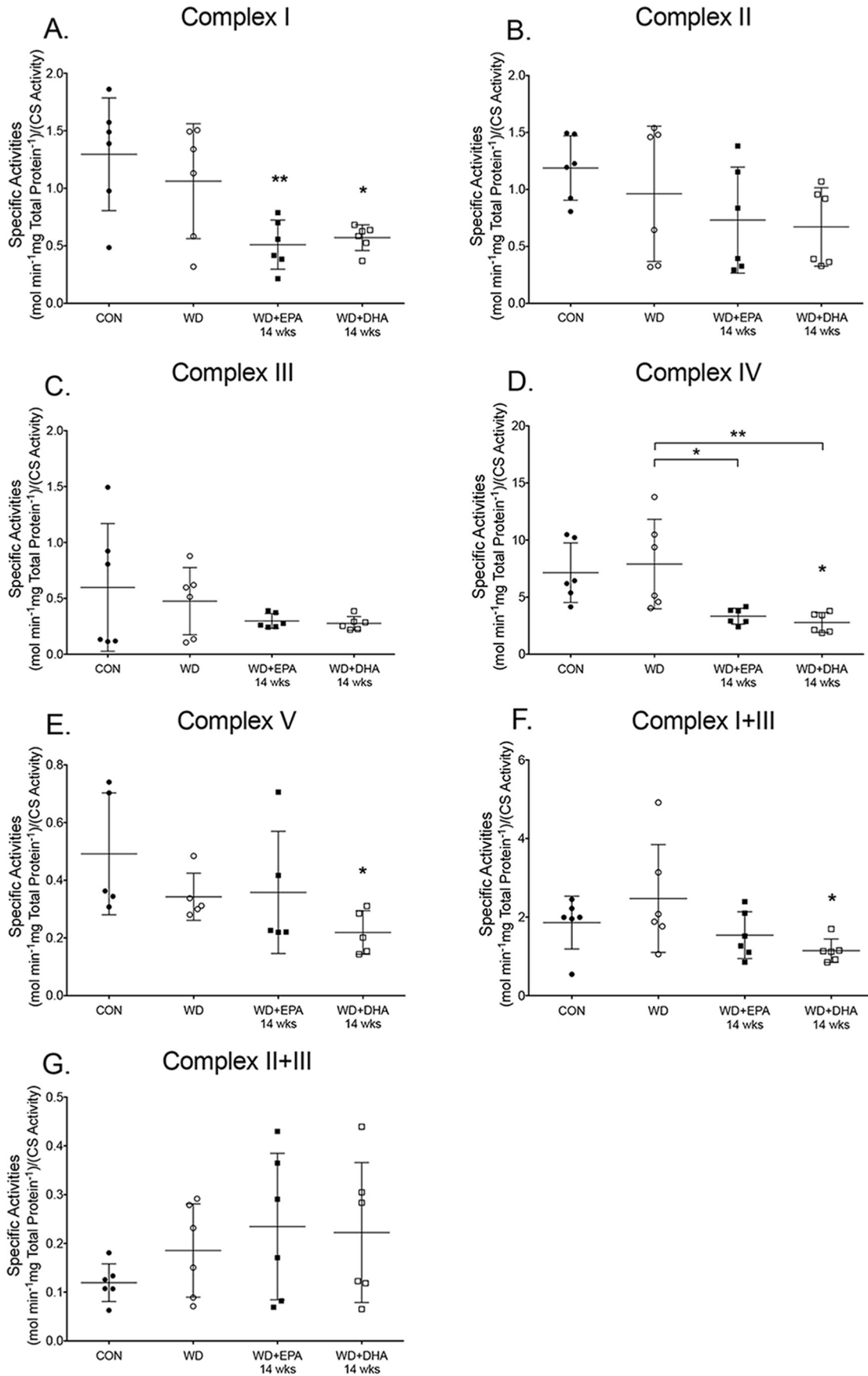
curves for LUVs containing $(18:2)_4CL$ relied on a one-site binding equation. The fitting revealed an equilibrium binding constant (K_d) of 1.8 ± 0.6 μM (Table 1), consistent with lipid-protein interactions at CL-specific binding sites.

$(18:2)_4CL$ rescues the major remodeling in the cardiolipin lipidome induced by long-term intake of DHA

The last set of experiments tested the possibility that the replacement of the predominant CL fatty acid, linoleic acid (18:2) with DHA (22:6), was driving the reduction in enzyme activity. Therefore, we fused cardiac mitochondria isolated from mice consuming the Western + DHA (14 weeks) diet with small unilamellar vesicles composed of $(18:2)_4CL$. We ensured that $(18:2)_4CL$ fusion did not influence the fatty acids associated with PC or PE. LC/MS heat maps show no alterations in any of the acyl chains associated with PC (Fig. S4A) and PE (Fig. S4B) upon fusion with $(18:2)_4CL$.

CL and MLCL were analyzed in response to the fusion. LC/MS analyses are presented as heat maps in Fig. 8 for CL species that were classified as either major (Fig. 8A), intermediate (Fig. 8B), or minor (Fig. 8C) in terms of abundance. MLCL was also analyzed (Fig. 8D). Several intermediate and minor CL species were altered in the $(18:2)_4CL$ mitochondrial fusion when compared with control and Western + DHA diets by 1.7–10.0-fold (Fig. 8, B and C). Notably, the most abundant CL species, $(18:2)_4$, was increased back to control levels with the fusion of $(18:2)_4CL$ by 12.6-fold relative to the Western + DHA (14 weeks) diet (Fig. 8A). In addition, fusion with $(18:2)_4CL$ increased $(18:1)(18:2)_3$ by 4.3-fold relative to the Western + DHA (14 weeks) diet (Fig. 8A). The fusion with $(18:2)_4CL$ also decreased several other CL species by 3.1–4.7-fold relative to the Western + DHA (14 weeks) diet (Fig. 8A). Relative to the control, fusion with $(18:2)_4CL$ still displayed decreased levels of some CL species such as $(18:1)(18:2)_3$ (Fig. 8A).

Cardiac mitochondrial complex I, IV, and V activities are rescued upon introduction of $(18:2)_4CL$ into the mitochondria of mice consuming DHA

We determined whether improvement in the CL lipidome of DHA-fed mice upon fusion of $(18:2)_4CL$ rescued the impaired oxidative phosphorylation enzyme activities. The fusion of $(18:2)_4CL$ to control samples had no effect on enzyme activity (data not shown). The fusion of $(18:2)_4CL$ to mitochondria isolated from Western + DHA (14 weeks) rescued complex I activity (Fig. 9A). The fusion of $(18:2)_4CL$ with the Western + DHA (14 weeks) diet did not influence complex II activity (Fig. 9B) and complex III activity was reduced relative to the control diet by 2.5-fold (Fig. 9C). $(18:2)_4CL$ fusion rescued complex IV and complex V activities by 2.4- and 2.5-fold relative to the Western + DHA diet (Fig. 9, D and E). Complex II and II + III activities

were not influenced by the introduction of $(18:2)_4CL$ (Fig. 9, F and G).

Discussion

The rationale for the study was based on previous data showing rearrangement of cardiac mitochondrial phospholipid acyl chains, particularly CL, in several diseases like cardiomyopathies and diabetes, as well as aging (8–11, 18). In such scenarios, decreased mitochondrial supercomplex formation, decreased mitochondrial respiratory function, increased oxidative stress, and elevated cardiac DHA acyl chains levels are generally observed (18, 45–54).

Herein, we first confirmed mouse studies by demonstrating that DHA levels were elevated in human type II diabetics. A limitation of this study was that we were not able to assay whether DHA was specifically associated with the polar lipid pool, particularly CL. This was due to a very limited tissue sample size obtained during surgery. Given that the concentration of free fatty acids is significantly low in the heart (55), it is likely that DHA levels represent polar and neutral lipids. We also acknowledge that the size of the samples, which were very difficult to obtain, was small. Thus, future studies will need to further confirm whether DHA levels, particularly in CL, are elevated in human subjects while controlling for various confounding variables.
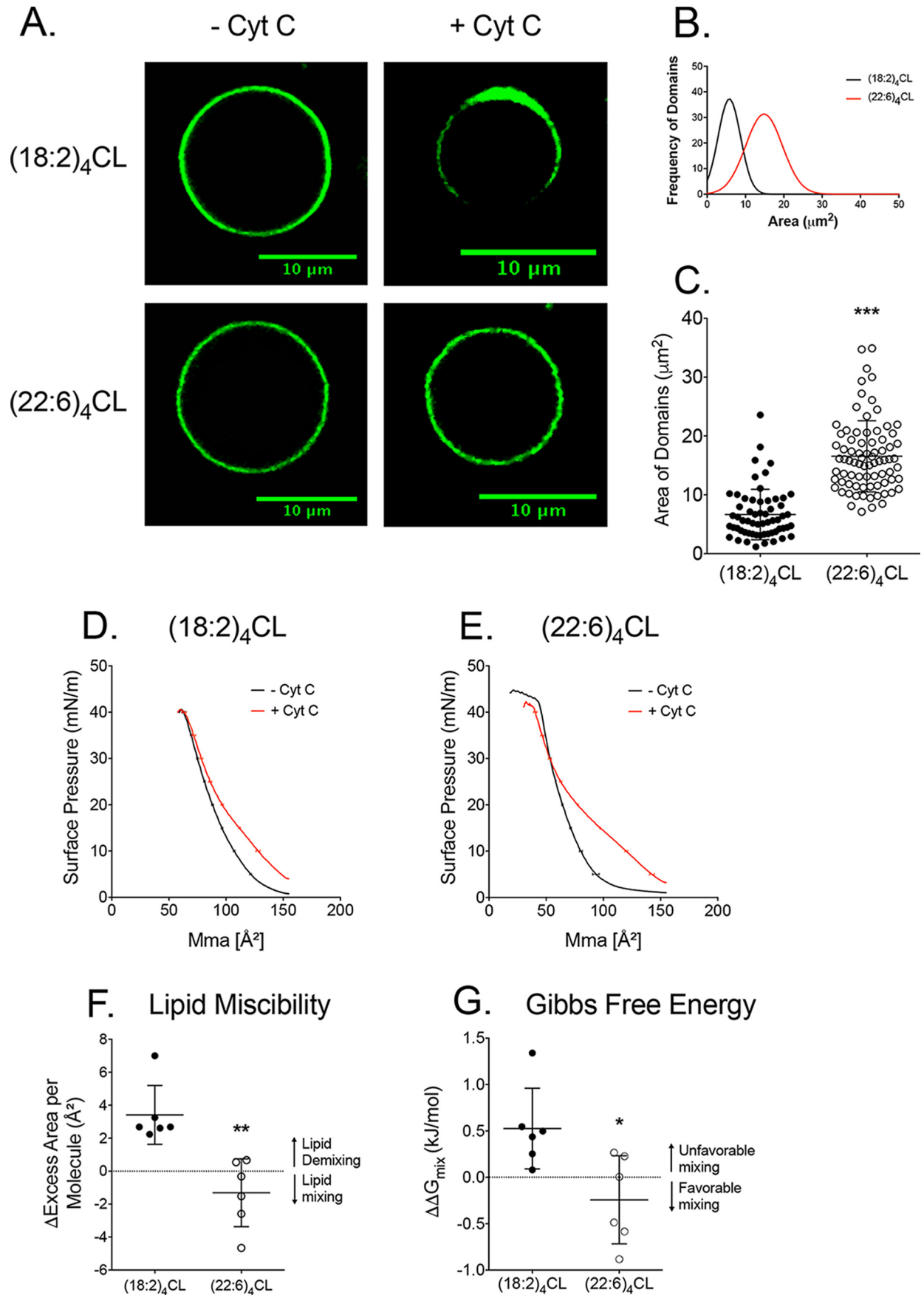
Following the human study, we performed experiments in a murine model to determine the potential underlying mechanisms by which DHA acyl chains influence mitochondrial enzymatic activity. A striking finding from the mouse study was that the Western diet in the absence of EPA or DHA dramatically remodeled the lipidome of the three major phospholipids of the mitochondria, but it had no effect on enzyme activity, even upon a strong reduction in $(18:2)_4CL$ levels. These results are in agreement with our previous work that showed a high fat diet had no influence on mouse cardiac enzyme activity upon moderate remodeling of phospholipids (56). In contrast, remodeling of the phospholipidome upon dietary supplementation with EPA and DHA led to diminished enzymatic activity of select complexes. These results were consistent with a study showing that fish oil can lower liver mitochondrial complex IV and V activities (57).

DHA potentially lowers cardiac mitochondrial enzyme activities by influencing domain organization and protein–lipid binding

The data suggest two potential mechanisms, which are not mutually exclusive, by which DHA lowered respiratory enzyme function. One possibility was that DHA prevented CL domain formation. Studies with biomimetic membranes specifically showed that $(22:6)_4CL$ had a stronger effect than $(18:2)_4CL$ on

Figure 5. EPA and DHA administration to a Western diet lowers select murine cardiac mitochondrial enzyme activities. *A,* complex I activity, measured by NADH oxidation for mice consuming a control (*CON*), Western diet (*WD*), WD + EPA, and WD + DHA. *B,* complex II activity, assessed by dichlorophenolindophenol reduction. *C,* complex III activity, assayed by cytochrome *c* reduction. *D,* complex IV activity, measured by cytochrome *c* oxidation. *E,* complex V activity, measured by the oxidation of NADH. *F,* complex I + III activity measured by NADH oxidation coupled to cytochrome *c* reduction. *G,* complex II + III activity assayed by succinate oxidation coupled to cytochrome *c* reduction. Activities were determined relative to total protein content and then normalized to citrate synthase (*CS*) activity. Data are the average ± S.D. from 5 to 6 independent experiments. *Asterisks* indicate significance from control (*, $p < 0.05$; **, $p < 0.01$). *Horizontal bars* with *asterisks* indicate significance between treatments.
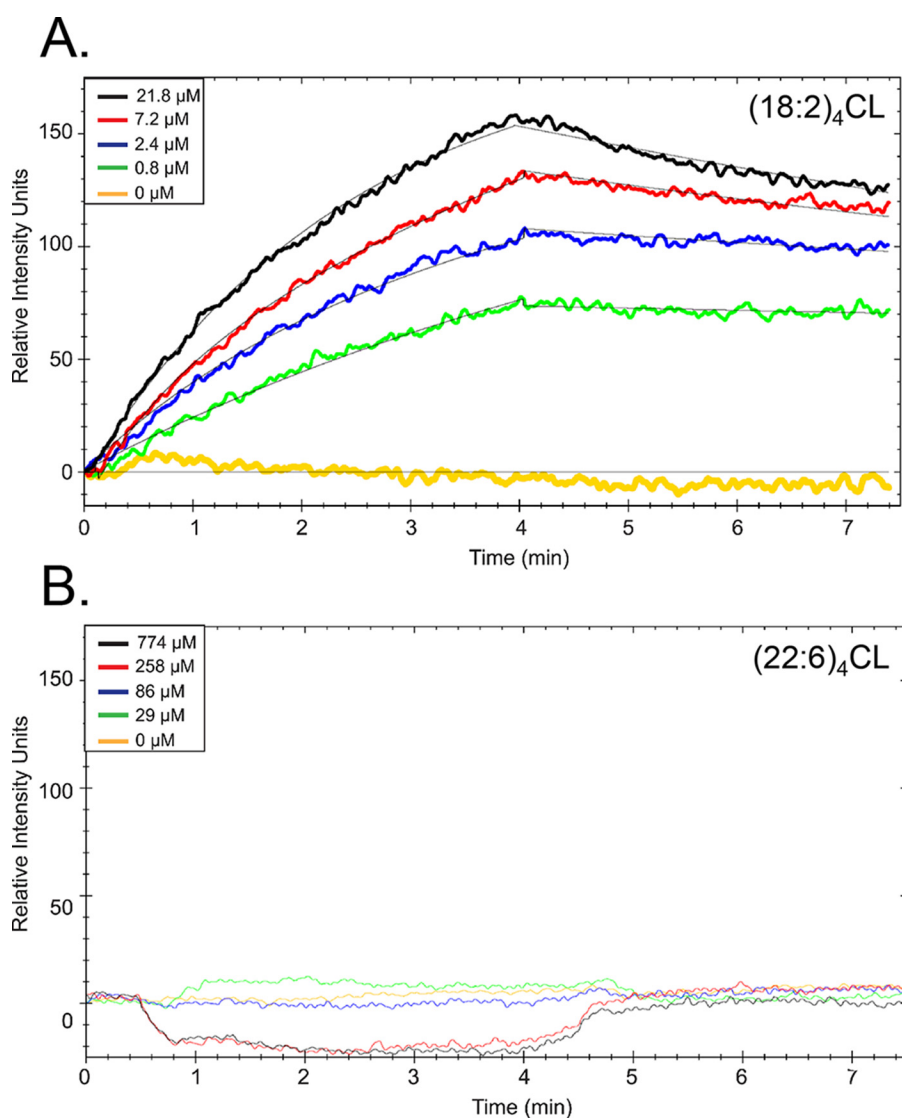
Figure 7. Replacement of (18:2)₄CL with (22:6)₄CL in biomimetic mitochondrial vesicles prevents binding to complex IV. Representative SPR sensorgrams of biomimetic LUVs containing $(18:2)_4$CL (*A*) or $(22:6)_4$CL (*B*) binding to complex IV are shown. LUVs modeled the composition of the inner mitochondrial membrane. Solubilized complex IV was immobilized to gold-plated carboxyl sensor chips using EDC/NHS chemistry (Nicoya Lifesciences). Binding of varying concentrations of LUVs were measured as a function of time. Small increases in the signals of $(22:6)_4$CL are attributed to non-specific binding interactions between the LUVs and sensor chip at high concentrations. Data in *A* were globally fit to a one-site binding model (*solid black line,* TraceDrawer) to determine k_{on}, k_{off}, and equilibrium dissociation constants. Binding constants (Table 1) were determined in three separate experiments using three different chips to account for chip-to-chip variability.

domain formation, which was driven by the ability of DHA acyl chains to promote phospholipid mixing. The other possibility was that DHA prevented binding of linoleic acyl chains to specific complexes.

There are several binding sites within complex I and IV that could be influenced by DHA. There are nine binding sites for CL in bovine complex I and depletion of CL from complex I

renders the enzyme inactive (24, 25). Similarly, CL is required for complex IV activity with four known CL-binding sites, two of which are considered high affinity. The high-affinity CL-binding sites are associated with the regulation of electron transport, and the loss of CL at these sites lowers enzymatic activity (26, 27). The two low-affinity sites are also important in the structural integrity of the complex in its dimer form (28, 58).

Figure 6. Replacement of (18:2)₄CL with (22:6)₄CL prevents formation of lipid domains due to a favorable Gibbs free energy of mixing. *A,* sample confocal images of biomimetic giant unilamellar vesicles containing either $(18:2)_4$CL or $(22:6)_4$CL. Cytochrome *c* (*Cyt C*) was added to promote phase separation, and images were visualized with the CL-specific probe NAO. Biomimetic membranes modeled the composition of the inner mitochondrial membrane. *B,* frequency distribution of the differing areas occupied by the NAO probe on the perimeter of the vesicles. A Gaussian fit was applied to the data. *C,* average area occupied by the NAO fluorophore measured with ImageJ software (National Institutes of Health). Each *dot* represents a single GUV. Monolayers were also constructed to assay lipid–lipid miscibility. Sample pressure–area isotherms of biomimetic monolayers are presented containing either $(18:2)_4$CL (*D*) or $(22:6)_4$CL (*E*). Lipid–lipid miscibility was quantified at a physiologically relevant surface pressure of 30 millinewtons (mN)/m in terms of the change in excess area per molecule (*F*) and Gibbs free energy (*G*) of mixing upon cytochrome *c* addition. Negative values for excess area per molecule and Gibbs free energy indicate favorable lipid–lipid mixing. Positive values indicate unfavorable mixing. Data are average ± S.D. from 3 to 6 independent experiments. *Asterisks* indicate statistical significance relative to $(18:2)_4$CL: *, $p < 0.05$; **, $p < 0.01$, *** $p < 0.001$.

⬚ASBMB

J. Biol. Chem. (2018) 293(2) 466–483 **475**

DHA remodels the cardiac lipidome to lower enzyme activity

Constant	$(18:2)_4CL$	$(22:6)_4CL$
k_{on}	$500 \pm 10 \text{ M}^{-1}\text{ s}^{-1}$	ND
k_{off}	$7.6 \pm 0.2 \ (\times 10^{-4}) \text{ s}^{-1}$	ND
K_d	$1.8 \pm 0.6 \ \mu\text{M}$	ND

Thus, DHA acyl chains may lower enzyme function due to diminished binding of linoleic acid to either of the two complexes. Indeed, studies to determine the strength of the phospholipid–protein interactions with complex IV revealed that biomimetic membranes containing $(22:6)_4CL$ did not bind to complex IV, whereas those containing $(18:2)_4CL$ exhibited significant interactions with complex IV (presumably both the low and high affinity CL-binding sites). Disruption of $(22:6)_4CL$ binding to complex IV could result in reduced conformational flexibility or electron transport, effectively reducing enzyme activity. Subsequent studies will need to test binding of other DHA-containing CL species with complex IV and other complexes. It was beyond the scope of this study to test CL-binding kinetics with all of the complexes.

Complex V activity was also lowered with DHA, which could be due to a specific disruption in CL domain formation. Complex V forms dimers, and CL is specifically needed to assemble the enzymes into larger oligomeric structures, which affects energy efficiency (16, 29, 59). It is possible that DHA, due to unique conformational flexibility, imparted disorder on the bilayer that leads to an impairment in the formation of higher order complex V oligomers that rely on the microdomain environment.

The effects of DHA on domain organization could also explain the reduction in complex I + III activity. Perhaps DHA lowered the ability of coenzyme q, the mobile electron carrier from complex I to complex III, to diffuse appropriately as the domains were disrupted. This would then explain why modifications to complex I and III activity alone did not recapitulate the results with complex I to III electron transfer. It is also conceivable that DHA impaired other aspects of membrane biophysical organization such as bending rigidity that could impede electron flow (60).

There are likely additional mechanisms by which DHA could lower respiratory enzyme function. These would include the possibility that an increase in acyl chain unsaturation with dietary DHA could manipulate CL turnover and thereby protein activity (61). In addition, DHA may have indirect effects on enzymatic responses by influencing the expression and activity of phospholipase $A_2\gamma$, which cleaves select fatty acids from CL to regulate mitochondrial bioenergetics (62).

Despite the clear impact that mitochondrial membrane phospholipidome remodeling was having on respiratory complex activity, it is noteworthy that coupled ADP-stimulated respiration was not altered with EPA and DHA (data not shown). This effect mirrored our previous study where EPA/DHA supplementation in high fat-fed mice did not significantly alter maximal respiration in the heart (63). This fact illustrates the

complexity of mitochondrial bioenergetics and suggests that although discrete respiratory complexes may be altered individually, or even in aggregate (*i.e.* supercomplexes), there are additional factors that impinge on respiratory function as a whole when mitochondria are intact and fully coupled. Altogether, the data provide a roadmap for future studies that will require purification of differing respiratory enzymes to study how DHA acyl chains disrupt enzyme activity in the context of CL-protein binding and formation of CL domains.

Paradox on DHA

In conditions such as obesity and type 2 diabetes, which are linked to cardiovascular diseases, pathological remodeling of CL with EPA and/or DHA increases oxidative damage that contributes to mitochondrial dysfunction (64). For instance, a study showed that DHA levels in C2C12 cells were elevated upon up-regulation of ALCAT1 (a lyso-CL acyltransferase), which remodels CL to species containing highly oxidizable acyl chains and increased oxidative stress (64). A deficiency in ALCAT1 in a murine model protected against diet-induced obesity and insulin resistance (64). Shotgun lipidomic studies by Han *et al.* (9, 18) also showed a significant decrease in CL abundance and a profound remodeling of the remaining CL species to include DHA acyl chains in rat diabetic myocardium.

In contrast, many studies demonstrate that consumption of EPA/DHA can have beneficial effects in obesity and type 2 diabetes through pleiotropic mechanisms. The mechanisms for improvements with EPA and DHA consist of enhancing insulin signaling, maintaining glucose metabolism, reversing dyslipidemia, and resolving inflammatory signals via targeting of transcription factors and gene expression (65–68). For instance, in a similar study by our group, supplementation of EPA and DHA in high-fat diet led to increased levels of 4-hydroxyhexenal adducts in the myocardium, products of EPA/DHA-specific lipid peroxidation (63). In parallel with the increase in hydroxyhexenal adducts, antioxidant gene expression increased while mitochondrial reactive oxygen species production decreased in the heart, suggesting that high-fat diet supplementation with EPA/DHA caused a beneficial "hormetic" response in the heart. Similar effects were also seen to some extent in a recent small clinical trial of fish oil in patients prior to cardiac surgery. Anderson *et al.* (69) showed that patients consuming 4 g/day of EPA/DHA ethyl esters (Lovaza™) had increased myocardial peroxisome proliferator-activated receptor-γ activation, up-regulated fatty acid metabolic gene expression, greater expression/activity of antioxidant as well as anti-inflammatory enzymes, and increased palmitoyl–carnitine-supported respiration.

Role of linoleic acid in the myocardium

Introduction of linoleic acid in CL vesicles rescued the decrement in the phospholipidomic profile and enzyme activities of complexes I, IV, and V in response to DHA. These results demonstrate mechanistically that it is not the loss of linoleic acid alone that drives the impairment in enzyme function because the Western diet alone did not impair enzyme activities. Instead, it was the replacement of linoleic acid with DHA that promoted the reduction in activities. The notable excep-
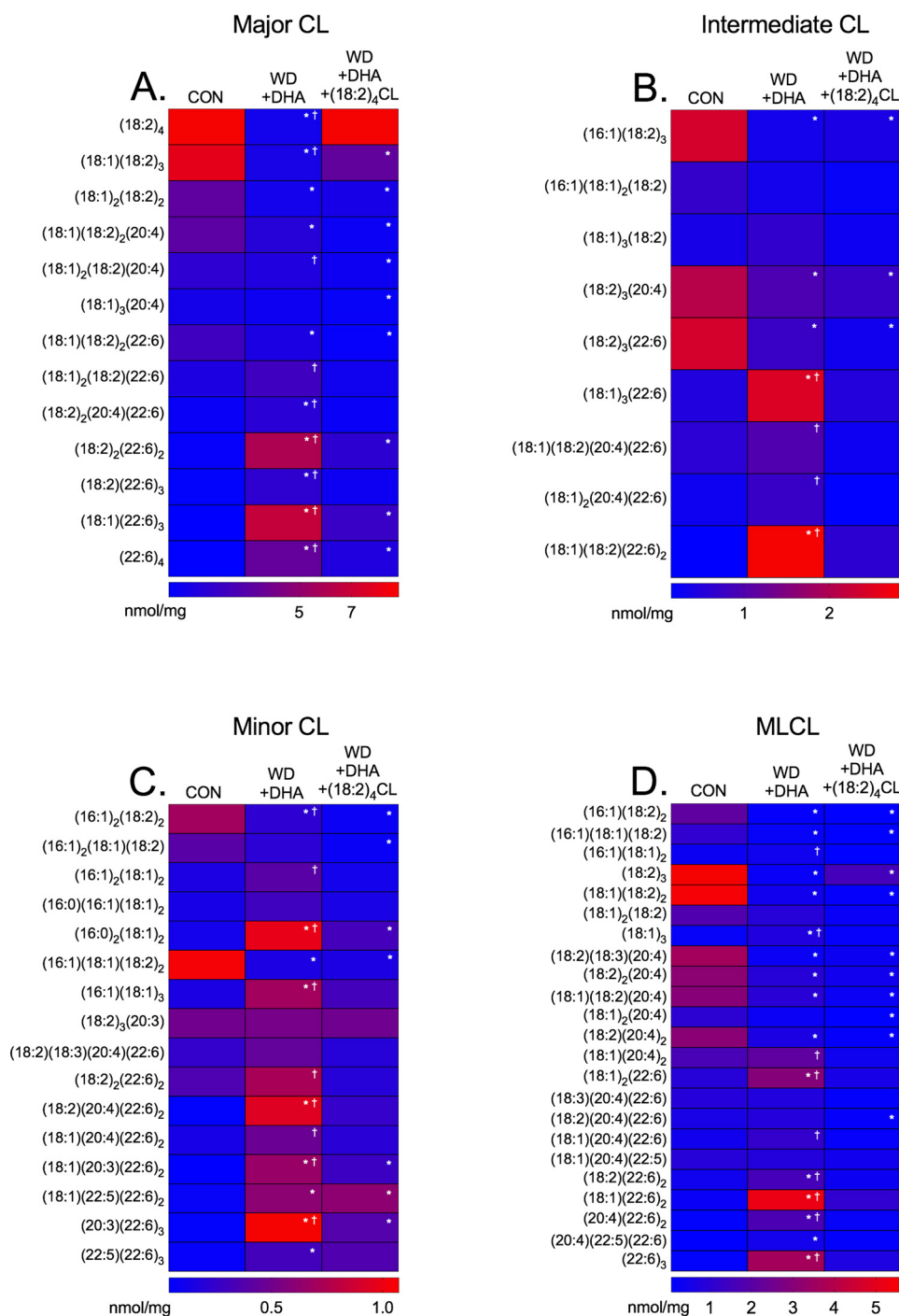
Figure 8. Incorporation of $(18:2)_4$CL improves the cardiolipin lipidome of mitochondria isolated from DHA-fed mice. Heat maps of major (*A*), intermediate (*B*), and minor (*C*) CL acyl chains for mice consuming a control (*CON*), Western diet (*WD*), and WD + DHA. *D*, monolyso-CL species in cardiac mitochondria are also shown. Data are the average $\pm$ S.E. from three independent experiments. *Asterisks* indicate significance from control (*, $p < 0.05$). *Daggers* indicate significance relative to WD + DHA + $(18:2)_4$CL (†, $p < 0.05$).

tion was complex III activity, which was not restored upon introduction of linoleic acid. Perhaps DHA was bound to complex III in a manner that precluded displacement by linoleic acid associated with CL. Several of the known complex III CL-specific bindings sites are buried deep within protein cavities, presumably making displacement of the DHA-containing CL difficult due to structural constraints (15).

The $(18:2)_4$CL rescue data advance the field by highlighting the importance of *n*-6 PUFAs in mitochondrial membranes.

There is considerable debate about the effects of *n*-6 PUFAs, notably linoleic acid, on cardiovascular health. Initially, linoleic acid was hypothesized to have benefits for cardiovascular outcomes because it lowers serum cholesterol (70, 71). However, recent studies challenge this notion about increasing the intake of linoleic acid at the expense of saturated fatty acids (72). For instance, several meta-analyses show that increasing the dietary consumption of *n*-6 PUFAs, at the expense of saturated fatty acids, does not lower the risk of death from cardiovascular dis-

ÁSBMB

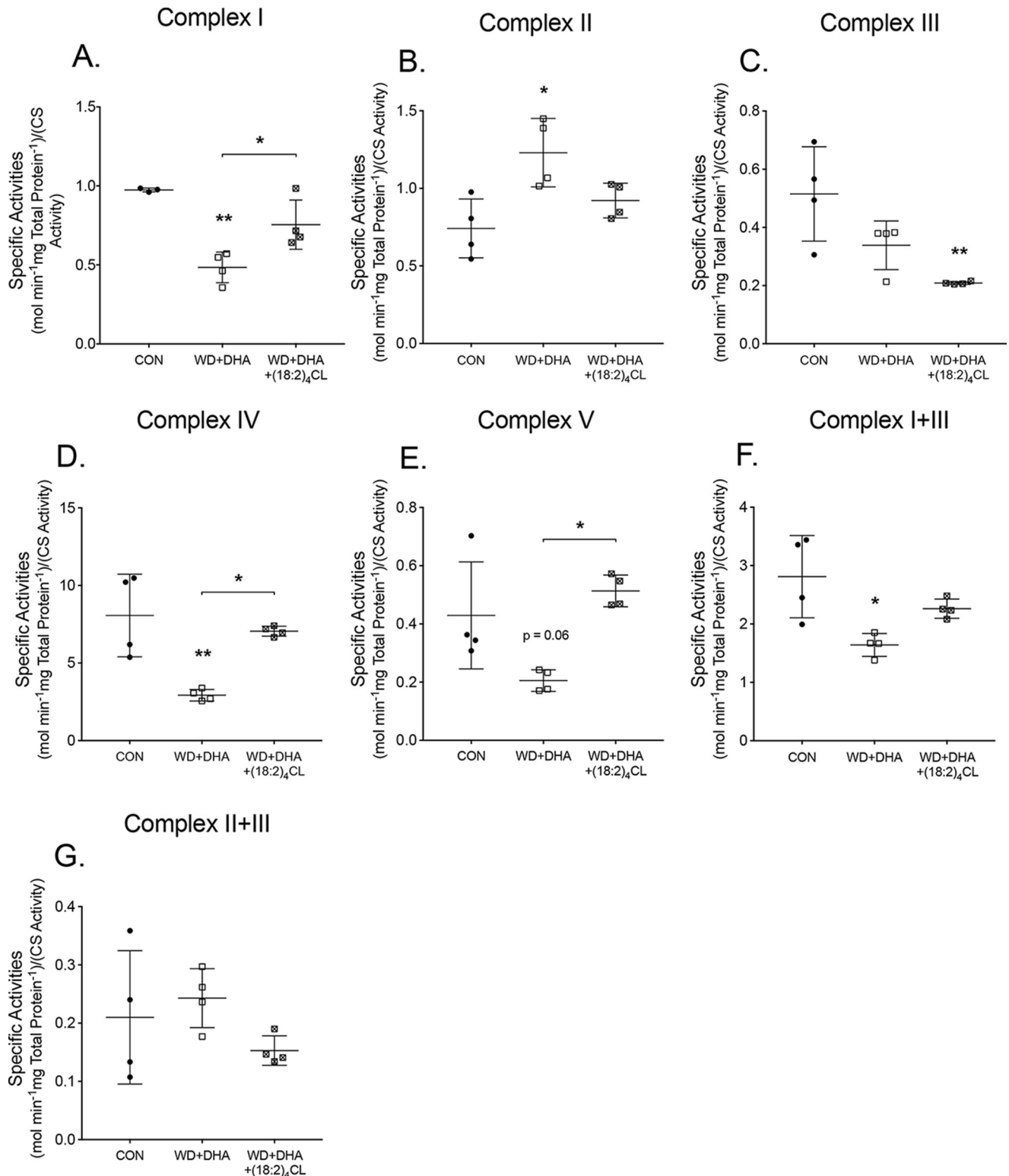*J. Biol. Chem.* (2018) 293(2) 466–483 **477**

Figure 9. (18:2)₄CL rescues the DHA-induced loss of complex I, IV, and V activities. *A,* complex I activity, measured by NADH oxidation for mice consuming a control (*CON*), Western diet (*WD*), and WD + DHA. *B,* complex II activity, measured by dichlorophenolindophenol reduction. *C,* complex III activity, assayed by cytochrome *c* reduction. *D,* complex IV activity, measured by cytochrome *c* oxidation. *E,* complex V activity, measured by the oxidation of NADH. *F,* complex I + III activity assayed by NADH oxidation coupled to cytochrome *c* reduction. *G,* complex II + III activity, assessed by succinate oxidation coupled to cytochrome *c* reduction. Activities were determined relative to total protein content and then normalized to citrate synthase (*CS*) activity. Data are the average ± S.E. from four independent experiments. *Asterisks* indicate significance from control (*, $p < 0.05$; **, $p < 0.01$). *Horizontal bars* with *asterisks* indicate significance between treatments.

eases (73–75). In addition to *n*-6 PUFAs, the role of *n*-3 PUFAs in cardiovascular diseases is still controversial. Meta-analyses on the consumption of EPA and DHA and coronary heart disease indicate that *n*-3 PUFAs may be associated with lowered cardiovascular risk (76, 77). However, a recent clinical trial showed that daily treatment with *n*-3 PUFAs did not decrease the prevalence of cardiovascular mortality or morbidity in patients with multiple cardiovascular risk factors (78). Our data suggest that linoleic acid is key for cardiac mitochondrial enzymatic activity, and its replacement, at least with select doses of DHA, could promote impairments.

It is conceivable that EPA and/or DHA could improve cardiac enzyme activities in other model systems. In this model, we did not find that DHA was improving fasting insulin or glucose clearance in contrast to other studies (33, 79). Thus, perhaps DHA could improve enzyme activities under conditions in which whole-body metabolism is improved. Furthermore, DHA in the triglyceride or free fatty acid form may have different effects on the mitochondrial phospholipidome and enzymatic activity, which was beyond the scope of this study.

Conclusions

The data demonstrate that remodeling of the murine cardiac mitochondrial phospholipidome in the absence of DHA had no influence on mitochondrial enzyme activities. In contrast, remodeling of the phospholipidome with DHA, in particular, leads to a reduction in complex I, IV, V, and I + III activities, potentially through mechanisms involving the formation of lipid domains and phospholipid–protein binding. These results suggest that increased levels of DHA in the myocardium in differing diseases may be targeting enzymatic activity. Furthermore, the impairments with DHA in the lipidome were generally rescued with the introduction of linoleic acid accompanied by an improvement in the activities of select complexes. This has implications for future studies on the balance between linoleic acid and *n*-3 PUFAs in the heart.

Experimental procedures

Human subjects

The Institutional Review Board of East Carolina University approved all aspects of human tissue and data collection for this study. The cohorts evaluated were type 2 diabetic and non-diabetic patients at Vidant Hospital undergoing elective coronary artery bypass graft surgery. The demographic and clinical data pertaining to the patients are shown in Table S1. The subjects were grouped either as non-diabetic or diabetic according to two major variables: 1) clinical diagnosis of diabetes; and 2) glycated hemoglobin (HbA$_{1c}$) values of ≥6.1 extending up to ~1 year prior to surgery. It is the standard of care at Vidant Hospital to give all diabetic patients intravenous insulin when admitted for surgery, and all other pre-operative diabetic medications are noted in Table S1. Patients with enlarged atria, history of arrhythmia, or left ventricular ejection fractions < 30% were excluded from this study.

Human atrial appendage biopsy, tissue processing, and fatty acid analyses

After median sternotomy, and prior to institution of cardiopulmonary bypass, a purse-string suture was placed in the right atrial appendage to allow for placement of the venous cannula. A sample of the appendage directly superior to the purse string was dissected and immediately rinsed in ice-cold saline to remove excess blood, trimmed of the epicardial layer and pericardial fat, and frozen in liquid N$_2$. Total fatty acids from the atrial appendage were extracted with organic solvents (HPLC grade, Sigma) and analyzed with gas chromatography as described previously (80). Stringent precautions were taken to prevent oxidation (80).

Animals and diets

All experiments were conducted in accordance with guidelines established by the Guide for the Care and Use of Laboratory Animals (National Institutes of Health Publication No. 85-23, revised 1996) and with prior approval by the Animal Care and Use Committee at East Carolina University and the University of North Carolina at Chapel Hill. Male C57BL/6 mice (Charles River, Wilmington, MA), 5 weeks old, were fed a low fat control diet, a Western diet (42% of kcal from milk fat), or a Western diet with 2% kcal from either EPA or DHA ethyl esters for 14 weeks (Envigo Inc., Indianapolis, IN). Short-term intervention with EPA and DHA was also tested, which entailed feeding mice the Western diet for 10 weeks followed by 4 weeks of the Western diet with either EPA or DHA. EPA and DHA ethyl esters (Cayman Chemicals, Ann Arbor, MI) were greater than 93% purity and were routinely tested for oxidation prior to and during the course of the study. The composition of the experimental diets is presented in Table S2. Mice were housed on a 12:12 h light/dark cycle with free access to water. Mice were sacrificed via isoflurane inhalation followed by cervical dislocation.

Metabolic profiling

Mice were fasted for 5 h prior to the administration of an intraperitoneal glucose injection (2.5 g/kg fat-free mass) of a 50% dextrose saline solution (Hospira Inc., Lake Forest, IL) (81). Blood glucose was monitored from the tail vein using an Alpha-Trak 2 animal glucometer (Abbott) at 0, 15, 30, 60, and 90 min post-injection (82). Values were normalized to fasting blood glucose levels, and glucose tolerance was assessed by calculating the corresponding area under the curve (AUC). Blood samples, collected after the 5-h fast using microcapillary tubes, were used to quantify insulin levels with an ultra-sensitive mouse insulin ELISA kit (Crystal Chem Inc., Downers Grove, IL). Fat and lean masses were determined with whole-body EchoMRI (Active Field Resources, LLC, Houston, TX).

Isolation of mitochondria

Mitochondrial isolations were performed on ice, and all instruments and buffers were chilled to 4 °C before isolation using our established protocols (56). Cardiac tissue was removed and rinsed in mitochondrial isolation medium (MIM) containing 300 mM sucrose, 10 mM Na-HEPES (pH 7.2), and 1

mM EGTA (Sigma). The tissue was minced for 5 min and diluted in MIM + BSA (1 mg/ml BSA) (pH 7.4). Tissue was then subjected to homogenization with a Teflon Potter homogenizer. The homogenate was centrifuged at $800 \times g$ for 10 min, and the supernatant was centrifuged at $12,000 \times g$ for 15 min. The mitochondrial pellet was resuspended in MIM and stored at -80 °C. Protein content was determined using a BCA protein quantification assay (Thermo Fisher Scientific, Waltham, MA).

Electrospray ionization mass spectrometry

Phospholipid molecular species were determined in lipid extracts (0.2 mg) of mitochondrial protein by liquid chromatography with electrospray ionization mass spectrometry (LC/MS) and analyzed as described previously (83).

Small unilamellar vesicle formation and fusion with mitochondria

SUVs were generated using 0.025 mg of $(18:2)_4$CL (Avanti Polar Lipids, Alabaster, AL) (84). Multilamellar vesicles (MLVs) were first constructed as shown previously (85). SUVs were then formed by the sonication of the MLVs using a Branson digital sonifier. SUVs were added to 1 mg of total mitochondrial protein and allowed to gently shake for an hour at 4 °C. Excess SUVs were then removed from the fused mitochondria, and the mitochondrial pellet was resuspended and stored at -80 °C.

Blue-native PAGE for quantifying supercomplex formation

Blue native-PAGE was performed as described previously (56). Briefly, pelleted mitochondria were resuspended in native-PAGE Sample Buffer (Life Technologies, Inc.) and solubilized using an 8:1 digitonin (Sigma) to protein ratio. After solubilization and centrifugation, the supernatants were collected and protein content was determined via a BCA protein quantification assay (Thermo Fisher Scientific). Samples were combined with 5% G-250 sample additive (Life Technologies, Inc.) and loaded onto the 3–12% BisTris gel (Life Technologies, Inc.). The gel was run on ice at 150 V for 3 h. Gels were fixed using 40% methanol and 10% acetic acid (Sigma) and destained in 8% acetic acid. Gels were imaged and quantified using the ChemiDoc Imaging System (Bio-Rad). Data were normalized to the total amount of protein in each sample.

Construction of biomimetic mitochondrial giant unilamellar vesicles (GUVs) to quantify domain organization

Biomimetic mitochondrial GUVs were constructed by co-dissolving lipids, 39.9 mol % 18:0–22:6 PC, 30.0 mol % 16:0–20:4 PE, 20 mol % $(18:2)_4$CL or $(22:6)_4$CL, 5 mol % 18:1–18:1 phosphatidylinositol (PI), 3 mol % 18:1–18:1 phosphatidylserine (PS), and 2 mol % cholesterol (Chol), with the CL-specific fluorescent probe nonyl acridine orange (NAO) (0.1 mol %), in chloroform (0.5 mg/ml). $(22:6)_4$CL was a custom synthesis from Avanti Polar Lipids. The levels of PC, PE, CL, PI, PS, and Chol approximated ratios found in the inner mitochondrial membrane. 5.0 μg of total lipid was spread onto the conductive side of an indium tin oxide-coated glass slide. The lipid-coated slide was subjected to dark vacuum overnight to remove excess sol-

vent. Once the lipid film was dried, a GUV electroformation chamber was assembled as described (86).

GUVs were constructed by electroformation at room temperature as described previously (39). To promote microdomain formation, cytochrome *c* was added at a 29:1 lipid to protein ratio. Following sample preparation, vesicles were drawn into a rectangular micro-capillary tube, mounted onto a microscope slide, and imaged at 23 °C.

Confocal microscopy and image analysis

Imaging was conducted with an Olympus FV1000 confocal microscope using a ×60 1.35NA oil immersion objective (Olympus, Waltham, MA). The NAO probe was excited with an argon laser at 488 nm. All acquired images were of GUV equatorial cross-sections. Analysis of lipid domains was conducted with ImageJ software (National Institutes of Health) as shown previously (39).

Quantification of the Gibbs free energy of lipid mixing

To quantify the Gibbs free energy of lipid–lipid mixing, biomimetic mitochondrial monolayers were generated by co-dissolving lipids (40 mol % 18:0–22:6 PC, 30.0 mol % 16:0–20:4 PE, 20 mol % $(18:2)_4$CL or $(22:6)_4$CL, 5 mol % 18:1–18:1PI, 3 mol % 18:1–18:1PS, and 2 mol % Chol) in chloroform (2.5 mg/ml). Lipid monolayers were constructed by spotting ~9.0 nmol on a subphase of 10 mM sodium phosphate buffer (pH 7.4). Biomimetic mitochondrial monolayers were analyzed in the absence and presence of cytochrome *c*. Excess chloroform was allowed to evaporate for 10 min prior to cytochrome addition and monolayer compression. Pressure-area isotherms were generated and analyzed as described previously (39). The excess area per molecule and Gibbs free energy were calculated to quantify lipid–lipid mixing and are presented as the change upon the addition of cytochrome *c* (39). All lipid mixtures were acquired multiple times to ensure reproducibility.

Synthesis of LUVs

LUVs were constructed at room temperature, as described previously (39), using the same lipid mixture described above for GUV and monolayer studies containing either $(18:2)_4$CL or $(22:6)_4$CL.

SPR

SPR data were recorded on an OpenSPR system (Nicoya Lifesciences). For all experiments, PBS (10 mM Na_2HPO_4, 2.7 mM KCl, and 137 mM NaCl, pH 7.4) was used as the running buffer. Solubilized complex IV in 25 mM Tris-HCl buffer (pH 7.8), 5 mM EDTA, and 39 mM *n*-dodecyl β-D-maltoside (Sigma) was diluted to 100 μg/ml in activation buffer and immobilized on a gold-plated carboxyl-functionalized nanosensor chip according to the manufacturer's instructions using carbodiimide cross-link chemistry (Nicoya Lifesciences). After immobilization and blocking (10 min), LUVs in differing concentrations were injected (200 μl) and allowed to interact with the sensor for 10 min at a pump speed of 20 μl/min. Complete dissociation of LUVs from the immobilized complex IV was observed after 15 min. Interactions between complex IV and the LUVs were determined in triplicate using three different chips to

eliminate the possibility of chip-to-chip variability. Sensorgrams obtained for the $(18:2)_4$CL were globally fit to a one-site binding model using TraceDrawer (Nicoya Lifesciences) to determine the association constant (k_{on}, $M^{-1} s^{-1}$), dissociation constant (k_{off}, s^{-1}), and the equilibrium binding constant (K_d, μM). Rate constants were obtained from global fits using 4–5 concentrations of LUVs and are presented as average ± S.D. from three separate experiments.

Mitochondrial kinetic assays

Kinetic assays were conducted using a UV-visible 1800 spectrophotometer at 37 °C as demonstrated previously (56). Complex I activity was measured by monitoring the oxidation of 0.8 mM NADH (Sigma) at 340 nm. Complex II activity was measured by the reduction of 80 μM dichlorophenolindophenol (Sigma) at 600 nm. Complex III activity was assayed by monitoring the reduction of 40 μM cytochrome c (Sigma) at 550 nm. Complex IV activity was measured by monitoring the oxidation of 10 μM reduced cytochrome c (Sigma) at 550 nm. Complex V activity was measured by the oxidation of 1 mM NADH (Sigma) at 340 nm. The activity of complexes I + III and II + III was measured by monitoring the reduction of 40 μM cytochrome c at 550 nm. Citrate synthase activity was assayed using 0.1 mM 5,5-dithiobis-(2-nitrobenzoic acid) (Sigma). Each reaction was performed in duplicate, and all activities were normalized to citrate synthase activity.

Statistical analyses

Data are presented as average ± S.D. All data are from multiple independent experiments, as indicated in the figure legends. Each independent experiment consisted of one mouse per diet group. The human data were analyzed with an unpaired one-tail t test because previous studies have established an increase in DHA levels in the myocardium (18); therefore, the null hypothesis for this study was set to test whether diabetics would increase DHA levels. The mouse data were normally distributed based on a Kolmogorov-Smirnov test. Thus, these results were analyzed with parametric statistics using GraphPad Prism 7 software. Statistical significance was established using a one-way analysis of variance followed by a post hoc Bonferroni test. $p < 0.05$ was considered significant.

References

1. Brown, D. A., Perry, J. B., Allen, M. E., Sabbah, H. N., Stauffer, B. L., Shaikh, S. R., Cleland, J. G., Colucci, W. S., Butler, J., Voors, A. A., Anker, S. D., Pitt, B., Pieske, B., Filippatos, G., Greene, S. J., and Gheorghiade, M. (2017) Expert consensus document: mitochondrial function as a therapeutic target in heart failure. *Nat. Rev. Cardiol.* **14,** 238–250 Medline
2. de Groot, H., and Rauen, U. (2007) Ischemia–reperfusion injury: processes in pathogenetic networks: a review. *Transplant. Proc.* **39,** 481–484 CrossRef Medline
3. Duncan, J. G. (2011) Mitochondrial dysfunction in diabetic cardiomyopathy. *Biochim. Biophys. Acta* **1813,** 1351–1359 CrossRef Medline
4. Hu, X., Bai, T., Xu, Z., Liu, Q., Zheng, Y., and Cai, L. (2017) Pathophysiological fundamentals of diabetic cardiomyopathy. *Compr. Physiol.* **7,** 693–711 Medline
5. Rosca, M. G., and Hoppel, C. L. (2013) Mitochondrial dysfunction in heart failure. *Heart Fail. Rev.* **18,** 607–622 CrossRef Medline
6. Sparagna, G. C., and Lesnefsky, E. J. (2009) Cardiolipin remodeling in the heart. *J. Cardiovasc. Pharmacol.* **53,** 290–301 CrossRef Medline
7. Schlame, M. (2013) Cardiolipin remodeling and the function of tafazzin. *Biochim. Biophys. Acta* **1831,** 582–588 CrossRef Medline
8. He, Q., and Han, X. (2014) Cardiolipin remodeling in diabetic heart. *Chem. Phys. Lipids* **179,** 75–81 CrossRef Medline
9. Han, X., Yang, J., Cheng, H., Yang, K., Abendschein, D. R., and Gross, R. W. (2005) Shotgun lipidomics identifies cardiolipin depletion in diabetic myocardium linking altered substrate utilization with mitochondrial dysfunction. *Biochemistry* **44,** 16684–16694 CrossRef Medline
10. Shi, Y. (2010) Emerging roles of cardiolipin remodeling in mitochondrial dysfunction associated with diabetes, obesity, and cardiovascular diseases. *J. Biomed. Res.* **24,** 6–15 CrossRef Medline
11. Gonzalvez, F., D'Aurelio, M., Boutant, M., Moustapha, A., Puech, J. P., Landes, T., Arnauné-Pelloquin, L., Vial, G., Taleux, N., Slomianny, C., Wanders, R. J., Houtkooper, R. H., Bellenguer, P., Møller, I. M., Gottlieb, E., *et al.* (2013) Barth syndrome: cellular compensation of mitochondrial dysfunction and apoptosis inhibition due to changes in cardiolipin remodeling linked to tafazzin (TAZ) gene mutation. *Biochim. Biophys. Acta* **1832,** 1194–1206 CrossRef Medline
12. Planas-Iglesias, J., Dwarakanath, H., Mohammadyani, D., Yanamala, N., Kagan, V. E., and Klein-Seetharaman, J. (2015) Cardiolipin interactions with proteins. *Biophys. J.* **109,** 1282–1294 CrossRef Medline
13. Paradies, G., Petrosillo, G., Pistolese, M., and Ruggiero, F. M. (2002) Reactive oxygen species affect mitochondrial electron transport complex I activity through oxidative cardiolipin damage. *Gene* **286,** 135–141 CrossRef Medline
14. Arnarez, C., Marrink, S. J., and Periole, X. (2013) Identification of cardiolipin binding sites on cytochrome c oxidase at the entrance of proton channels. *Sci. Rep.* **3,** 1263 CrossRef Medline
15. Arnarez, C., Mazat, J. P., Elezgaray, J., Marrink, S. J., and Periole, X. (2013) Evidence for cardiolipin binding sites on the membrane-exposed surface of the cytochrome bc1. *J. Am. Chem. Soc.* **135,** 3112–3120 CrossRef Medline
16. Eble, K. S., Coleman, W. B., Hantgan, R. R., and Cunningham, C. C. (1990) Tightly associated cardiolipin in the bovine heart mitochondrial ATP synthase as analyzed by ^{31}P nuclear magnetic resonance spectroscopy. *J. Biol. Chem.* **265,** 19434–19440 Medline
17. Iverson, S. L., and Orrenius, S. (2004) The cardiolipin-cytochrome c interaction and the mitochondrial regulation of apoptosis. *Arch. Biochem. Biophys.* **423,** 37–46 CrossRef Medline
18. Han, X., Yang, J., Yang, K., Zhao, Z., Abendschein, D. R., and Gross, R. W. (2007) Alterations in myocardial cardiolipin content and composition occur at the very earliest stages of diabetes: a shotgun lipidomics study. *Biochemistry* **46,** 6417–6428 CrossRef Medline
19. Endo, J., and Arita, M. (2016) Cardioprotective mechanism of omega-3 polyunsaturated fatty acids. *J. Cardiol.* **67,** 22–27 CrossRef Medline
20. Madingou, N., Gilbert, K., Tomaro, L., Prud'homme Touchette, C., Trudeau, F., Fortin, S., and Rousseau, G. (2016) Comparison of the effects of EPA and DHA alone or in combination in a murine model of myocardial infarction. *Prostaglandins Leukot. Essent. Fatty Acids* **111,** 11–16 CrossRef Medline
21. Rangel-Huerta, O. D., and Gil, A. (2017) Omega 3 fatty acids in cardiovascular disease risk factors: an updated systematic review of randomised clinical trials. *Clin. Nutr.* **2017,** S0261-S5614 Medline

22. Jeckel, K. M., Veeramachaneni, D. N., Chicco, A. J., Chapman, P. L., Mulligan, C. M., Hegarty, J. R., Pagliassotti, M. J., Ferguson, L. A., Bouma, G. J., and Frye, M. A. (2012) Docosahexaenoic acid supplementation does not improve Western diet-induced cardiomyopathy in rats. *PLoS ONE* **7,** e51994 CrossRef Medline

23. Horvath, S. E., and Daum, G. (2013) Lipids of mitochondria. *Prog. Lipid Res.* **52,** 590–614 CrossRef Medline

24. Sharpley, M. S., Shannon, R. J., Draghi, F., and Hirst, J. (2006) Interactions between phospholipids and NADH:ubiquinone oxidoreductase (complex I) from bovine mitochondria. *Biochemistry* **45,** 241–248 CrossRef Medline

25. Fry, M., and Green, D. E. (1981) Cardiolipin requirement for electron transfer in complex I and III of the mitochondrial respiratory chain. *J. Biol. Chem.* **256,** 1874–1880 Medline

26. Robinson, N. C. (1993) Functional binding of cardiolipin to cytochrome c oxidase. *J. Bioenerg. Biomembr.* **25,** 153–163 CrossRef Medline

27. Robinson, N. C. (1982) Specificity and binding affinity of phospholipids to the high-affinity cardiolipin sites of beef heart cytochrome c oxidase. *Biochemistry* **21,** 184–188 CrossRef Medline

28. Sedlák, E., and Robinson, N. C. (1999) Phospholipase A(2) digestion of cardiolipin bound to bovine cytochrome c oxidase alters both activity and quaternary structure. *Biochemistry* **38,** 14966–14972 CrossRef Medline

29. Acehan, D., Malhotra, A., Xu, Y., Ren, M., Stokes, D. L., and Schlame, M. (2011) Cardiolipin affects the supramolecular organization of ATP synthase in mitochondria. *Biophys. J.* **100,** 2184–2192 CrossRef Medline

30. Zhang, M., Mileykovskaya, E., and Dowhan, W. (2002) Gluing the respiratory chain together. Cardiolipin is required for supercomplex formation in the inner mitochondrial membrane. *J. Biol. Chem.* **277,** 43553–43556 CrossRef Medline

31. Zhang, M., Mileykovskaya, E., and Dowhan, W. (2005) Cardiolipin is essential for organization of complexes III and IV into a supercomplex in intact yeast mitochondria. *J. Biol. Chem.* **280,** 29403–29408 CrossRef Medline

32. Maniti, O., Lecompte, M. F., Marcillat, O., Desbat, B., Buchet, R., Vial, C., and Granjon, T. (2009) Mitochondrial creatine kinase binding to phospholipid monolayers induces cardiolipin segregation. *Biophys. J.* **96,** 2428–2438 CrossRef Medline

33. Pinel, A., Pitois, E., Rigaudiere, J. P., Jouve, C., De Saint-Vincent, S., Laillet, B., Montaurier, C., Huertas, A., Morio, B., and Capel, F. (2016) EPA prevents fat mass expansion and metabolic disturbances in mice fed with a Western diet. *J. Lipid Res.* **57,** 1382–1397 CrossRef Medline

34. Lenaz, G., Baracca, A., Barbero, G., Bergamini, C., Dalmonte, M. E., Del Sole, M., Faccioli, M., Falasca, A., Fato, R., Genova, M. L., Sgarbi, G., and Solaini, G. (2010) Mitochondrial respiratory chain super-complex I–III in physiology and pathology. *Biochim. Biophys. Acta* **1797,** 633–640 CrossRef Medline

35. Acín-Pérez, R., Fernández-Silva, P., Peleato, M. L., Pérez-Martos, A., and Enriquez, J. A. (2008) Respiratory active mitochondrial supercomplexes. *Mol. Cell* **32,** 529–539 CrossRef Medline

36. Epand, R. F., Tokarska-Schlattner, M., Schlattner, U., Wallimann, T., and Epand, R. M. (2007) Cardiolipin clusters and membrane domain formation induced by mitochondrial proteins. *J. Mol. Biol.* **365,** 968–980 CrossRef Medline

37. Beales, P. A., Bergstrom, C. L., Geerts, N., Groves, J. T., and Vanderlick, T. K. (2011) Single vesicle observations of the cardiolipin-cytochrome c interaction: induction of membrane morphology changes. *Langmuir* **27,** 6107–6115 CrossRef Medline

38. Feigenson, G. W. (2009) Phase diagrams and lipid domains in multicomponent lipid bilayer mixtures. *Biochim. Biophys. Acta* **1788,** 47–52 CrossRef Medline

39. Pennington, E. R., Fix, A., Sullivan, E. M., Brown, D. A., Kennedy, A., and Shaikh, S. R. (2017) Distinct membrane properties are differentially influenced by cardiolipin content and acyl chain composition in biomimetic membranes. *Biochim. Biophys. Acta* **1859,** 257–267 CrossRef Medline

40. Paradies, G., Paradies, V., De Benedictis, V., Ruggiero, F. M., and Petrosillo, G. (2014) Functional role of cardiolipin in mitochondrial bioenergetics. *Biochim. Biophys. Acta* **1837,** 408–417 CrossRef Medline

41. Hodnik, V., and Anderluh, G. (2013) Surface plasmon resonance for measuring interactions of proteins with lipid membranes. *Methods Mol. Biol.* **974,** 23–36 CrossRef Medline

42. Abramovitch, D. A., Marsh, D., and Powell, G. L. (1990) Activation of beef-heart cytochrome c oxidase by cardiolipin and analogues of cardiolipin. *Biochim. Biophys. Acta* **1020,** 34–42 CrossRef Medline

43. Robinson, N. C., Zborowski, J., and Talbert, L. H. (1990) Cardiolipin-depleted bovine heart cytochrome c oxidase: binding stoichiometry and affinity for cardiolipin derivatives. *Biochemistry* **29,** 8962–8969 CrossRef Medline

44. Paradies, G., Petrosillo, G., and Ruggiero, F. M. (1997) Cardiolipin-dependent decrease of cytochrome c oxidase activity in heart mitochondria from hypothyroid rats. *Biochim. Biophys. Acta* **1319,** 5–8 CrossRef Medline

45. Sparagna, G. C., Chicco, A. J., Murphy, R. C., Bristow, M. R., Johnson, C. A., Rees, M. L., Maxey, M. L., McCune, S. A., and Moore, R. L. (2007) Loss of cardiac tetralinoleoyl cardiolipin in human and experimental heart failure. *J. Lipid Res.* **48,** 1559–1570 CrossRef Medline

46. Petrosillo, G., Di Venosa, N., Ruggiero, F. M., Pistolese, M., D'Agostino, D., Tiravanti, E., Fiore, T., and Paradies, G. (2005) Mitochondrial dysfunction associated with cardiac ischemia/reperfusion can be attenuated by oxygen tension control. Role of oxygen-free radicals and cardiolipin. *Biochim. Biophys. Acta* **1710,** 78–86 CrossRef Medline

47. Rosca, M. G., Vazquez, E. J., Kerner, J., Parland, W., Chandler, M. P., Stanley, W., Sabbah, H. N., and Hoppel, C. L. (2008) Cardiac mitochondria in heart failure: decrease in respirasomes and oxidative phosphorylation. *Cardiovasc. Res.* **80,** 30–39 CrossRef Medline

48. Genova, M. L., and Lenaz, G. (2015) The interplay between respiratory supercomplexes and ROS in aging. *Antioxid. Redox Signal.* **23,** 208–238 CrossRef Medline

49. Lee, H. J., Mayette, J., Rapoport, S. I., and Bazinet, R. P. (2006) Selective remodeling of cardiolipin fatty acids in the aged rat heart. *Lipids Health. Dis.* **5,** 2 CrossRef Medline

50. Gómez, L. A., Monette, J. S., Chavez, J. D., Maier, C. S., and Hagen, T. M. (2009) Supercomplexes of the mitochondrial electron transport chain decline in the aging rat heart. *Arch. Biochem. Biophys.* **490,** 30–35 CrossRef Medline

51. Vreken, P., Valianpour, F., Nijtmans, L. G., Grivell, L. A., Plecko, B., Wanders, R. J., and Barth, P. G. (2000) Defective remodeling of cardiolipin and phosphatidylglycerol in Barth syndrome. *Biochem. Biophys. Res. Commun.* **279,** 378–382 CrossRef Medline

52. Schlame, M., Towbin, J. A., Heerdt, P. M., Jehle, R., DiMauro, S., and Blanck, T. J. (2002) Deficiency of tetralinoleoyl-cardiolipin in Barth syndrome. *Ann. Neurol.* **51,** 634–637 CrossRef Medline

53. McKenzie, M., Lazarou, M., Thorburn, D. R., and Ryan, M. T. (2006) Mitochondrial respiratory chain supercomplexes are destabilized in Barth syndrome patients. *J. Mol. Biol.* **361,** 462–469 CrossRef Medline

54. Kiebish, M. A., Yang, K., Liu, X., Mancuso, D. J., Guan, S., Zhao, Z., Sims, H. F., Cerqua, R., Cade, W. T., Han, X., and Gross, R. W. (2013) Dysfunctional cardiac mitochondrial bioenergetic, lipidomic, and signaling in a murine model of Barth syndrome. *J. Lipid Res.* **54,** 1312–1325 CrossRef Medline

55. Wheeldon, L. W., Schumert, Z., and Turner, D. A. (1965) Lipid composition of heart muscle homogenate. *J. Lipid Res.* **6,** 481–489 Medline

56. Sullivan, E. M., Fix, A., Crouch, M. J., Sparagna, G. C., Zeczycki, T. N., Brown, D. A., and Shaikh, S. R. (2017) Murine diet-induced obesity remodels cardiac and liver mitochondrial phospholipid acyl chains with differential effects on respiratory enzyme activity. *J. Nutr. Biochem.* **45,** 94–103 CrossRef Medline

57. Aoun, M., Feillet-Coudray, C., Fouret, G., Chabi, B., Crouzier, D., Ferreri, C., Chatgilialoglu, C., Wrutniak-Cabello, C., Cristol, J. P., Carbonneau, M. A., and Coudray, C. (2012) Rat liver mitochondrial membrane characteristics and mitochondrial functions are more profoundly altered by dietary lipid quantity than by dietary lipid quality: effect of different nutritional lipid patterns. *Br. J. Nutr.* **107,** 647–659 CrossRef Medline

58. Sedlák, E., Panda, M., Dale, M. P., Weintraub, S. T., and Robinson, N. C. (2006) Photolabeling of cardiolipin binding subunits within bovine heart cytochrome c oxidase. *Biochemistry* **45,** 746–754 CrossRef Medline

ASBMB

59. Paumard, P., Vaillier, J., Coulary, B., Schaeffer, J., Soubannier, V., Mueller, D. M., Brèthes, D., di Rago, J. P., and Velours, J. (2002) The ATP synthase is involved in generating mitochondrial cristae morphology. *EMBO J.* **21,** 221–230 CrossRef Medline

60. Shindou, H., Koso, H., Sasaki, J., Nakanishi, H., Sagara, H., Nakagawa, K. M., Takahashi, Y., Hishikawa, D., Iizuka-Hishikawa, Y., Tokumasu, F., Noguchi, H., Watanabe, S., Sasaki, T., and Shimizu, T. (2017) Docosahexaenoic acid preserves visual function by maintaining correct disc morphology in retinal photoreceptor cells. *J. Biol. Chem.* **292,** 12054–12064 CrossRef Medline

61. Xu, Y., Phoon, C. K., Berno, B., D'Souza, K., Hoedt, E., Zhang, G., Neubert, T. A., Epand, R. M., Ren, M., and Schlame, M. (2016) Loss of protein association causes cardiolipin degradation in Barth syndrome. *Nat. Chem. Biol.* **12,** 641–647 CrossRef Medline

62. Liu, G. Y., Moon, S. H., Jenkins, C. M., Li, M., Sims, H. F., Guan, S., and Gross, R. W. (2017) The phospholipase iPLA2γ is a major mediator releasing oxidized aliphatic chains from cardiolipin, integrating mitochondrial bioenergetics and signaling. *J. Biol. Chem.* **292,** 10672–10684 CrossRef Medline

63. Anderson, E. J., Thayne, K., Harris, M., Carraway, K., and Shaikh, S. R. (2012) Aldehyde stress and up-regulation of Nrf2-mediated antioxidant systems accompany functional adaptations in cardiac mitochondria from mice fed *n*-3 polyunsaturated fatty acids. *Biochem. J.* **441,** 359–366 CrossRef Medline

64. Li, J., Romestaing, C., Han, X., Li, Y., Hao, X., Wu, Y., Sun, C., Liu, X., Jefferson, L. S., Xiong, J., Lanoue, K. F., Chang, Z., Lynch, C. J., Wang, H., and Shi, Y. (2010) Cardiolipin remodeling by ALCAT1 links oxidative stress and mitochondrial dysfunction to obesity. *Cell Metab.* **12,** 154–165 CrossRef Medline

65. Liu, X., Xue, Y., Liu, C., Lou, Q., Wang, J., Yanagita, T., Xue, C., and Wang, Y. (2013) Eicosapentaenoic acid-enriched phospholipid ameliorates insulin resistance and lipid metabolism in diet-induced obese mice. *Lipids Health Dis.* **12,** 109 Medline

66. Nettleton, J. A., and Katz, R. (2005) *n*-3 long-chain polyunsaturated fatty acids in type 2 diabetes: a review. *J. Am. Diet. Assoc.* **105,** 428–440 CrossRef Medline

67. Lorente-Cebriá, S., Costa, A. G., Navas-Carretero, S., Zabala, M., Martínez, J. A., and Moreno-Aliaga, M. J. (2013) Role of omega-3 fatty acids in obesity, metabolic syndrome, and cardiovascular diseases: a review of the evidence. *J. Physiol. Biochem.* **69,** 633–651 CrossRef Medline

68. Lombardo, Y. B., Hein, G., and Chicco, A. (2007) Metabolic syndrome: effects of *n*-3 PUFAs on a model of dyslipidemia, insulin resistance and adiposity. *Lipids* **42,** 427–437 CrossRef Medline

69. Anderson, E. J., Thayne, K. A., Harris, M., Shaikh, S. R., Darden, T. M., Lark, D. S., Williams, J. M., Chitwood, W. R., Kypson, A. P., and Rodriguez, E. (2014) Do fish oil omega-3 fatty acids enhance antioxidant capacity and mitochondrial fatty acid oxidation in human atrial myocardium via PPARγ activation? *Antioxid. Redox Signal.* **21,** 1156–1163 CrossRef Medline

70. Katan, M. B., Zock, P. L., and Mensink, R. P. (1995) Dietary oils, serum lipoproteins, and coronary heart disease. *Am. J. Clin. Nutr.* **61,** 1368S-1373S Medline

71. Frantz, I. D., Jr, Dawson, E. A., Ashman, P. L., Gatewood, L. C., Bartsch, G. E., Kuba, K., and Brewer, E. R. (1989) Test of effect of lipid lowering by diet on cardiovascular risk. The Minnesota Coronary Survey. *Arteriosclerosis* **9,** 129–135 CrossRef Medline

72. Harris, W. S., Mozaffarian, D., Rimm, E., Kris-Etherton, P., Rudel, L. L., Appel, L. J., Engler, M. M., Engler, M. B., and Sacks, F. (2009) Omega-6 fatty acids and risk for cardiovascular disease: a science advisory from the American Heart Association Nutrition Subcommittee of the Council on Nutrition, Physical Activity, and Metabolism; Council on Cardiovascular Nursing; and Council on Epidemiology and Prevention. *Circulation* **119,** 902–907 CrossRef Medline

73. Ramsden, C. E., Zamora, D., Leelarthaepin, B., Majchrzak-Hong, S. F., Faurot, K. R., Suchindran, C. M., Ringel, A., Davis, J. M., and Hibbeln, J. R. (2013) Use of dietary linoleic acid for secondary prevention of coronary heart disease and death: evaluation of recovered data from the Sydney Diet Heart Study and updated meta-analysis. *BMJ* **346,** e8707 CrossRef Medline

74. Ramsden, C. E., Zamora, D., Majchrzak-Hong, S., Faurot, K. R., Broste, S. K., Frantz, R. P., Davis, J. M., Ringel, A., Suchindran, C. M., and Hibbeln, J. R. (2016) Re-evaluation of the traditional diet-heart hypothesis: analysis of recovered data from Minnesota Coronary Experiment (1968–73). *BMJ* **353,** 1246 CrossRef Medline

75. Chowdhury, R., Warnakula, S., Kunutsor, S., Crowe, F., Ward, H. A., Johnson, L., Franco, O. H., Butterworth, A. S., Forouhi, N. G., Thompson, S. G., Khaw, K. T., Mozaffarian, D., Danesh, J., and Di Angelantonio, E. (2014) Association of dietary, circulating, and supplement fatty acids with coronary risk: a systematic review and meta-analysis. *Ann. Intern. Med.* **160,** 398–406 CrossRef Medline

76. Alexander, D. D., Miller, P. E., Van Elswyk, M. E., Kuratko, C. N., and Bylsma, L. C. (2017) A meta-analysis of randomized controlled trials and prospective cohort studies of eicosapentaenoic and docosahexaenoic long-chain omega-3 fatty acids and coronary heart disease risk. *Mayo Clin. Proc.* **92,** 15–29 CrossRef Medline

77. Harris, W. S., Del Gobbo, L., and Tintle, N. L. (2017) The omega-3 index and relative risk for coronary heart disease mortality: estimation from 10 cohort studies. *Atherosclerosis* **262,** 51–54 CrossRef Medline

78. Risk and Prevention Study Collaborative Group, Roncaglioni, M. C., Tombesi, M., Avanzini, F., Barlera, S., Caimi, V., Longoni, P., Marzona, I., Milani, V., Silletta, M. G., Tognoni, G., and Marchioli, R. (2013) *n*-3 fatty acids in patients with multiple cardiovascular risk factors. *N. Engl. J. Med.* **368,** 1800–1808 CrossRef Medline

79. LeMieux, M. J., Kalupahana, N. S., Scoggin, S., and Moustaid-Moussa, N. (2015) Eicosapentaenoic acid reduces adipocyte hypertrophy and inflammation in diet-induced obese mice in an adiposity-independent manner. *J. Nutr.* **145,** 411–417 CrossRef Medline

80. Rockett, B. D., Teague, H., Harris, M., Melton, M., Williams, J., Wassall, S. R., and Shaikh, S. R. (2012) Fish oil increases raft size and membrane order of B cells accompanied by differential effects on function. *J. Lipid Res.* **53,** 674–685 CrossRef Medline

81. McGuinness, O. P., Ayala, J. E., Laughlin, M. R., and Wasserman, D. H. (2009) NIH experiment in centralized mouse phenotyping: the Vanderbilt experience and recommendations for evaluating glucose homeostasis in the mouse. *Am. J. Physiol. Endocrinol. Metab.* **297,** E849–E855 CrossRef Medline

82. Kosaraju, R., Guesdon, W., Crouch, M. J., Teague, H. L., Sullivan, E. M., Karlsson, E. A., Schultz-Cherry, S., Gowdy, K., Bridges, L. C., Reese, L. R., Neufer, P. D., Armstrong, M., Reisdorph, N., Milner, J. J., Beck, M., and Shaikh, S. R. (2017) B cell activity is impaired in human and mouse obesity and is responsive to an essential fatty acid upon murine influenza infection. *J. Immunol.* **198,** 4738–4752 CrossRef Medline

83. Sparagna, G. C., Johnson, C. A., McCune, S. A., Moore, R. L., and Murphy, R. C. (2005) Quantitation of cardiolipin molecular species in spontaneously hypertensive heart failure rats using electrospray ionization mass spectrometry. *J. Lipid Res.* **46,** 1196–1204 CrossRef Medline

84. Shaikh, S. R., Sullivan, E. M., Alleman, R. J., Brown, D. A., and Zeczycki, T. N. (2014) Increasing mitochondrial membrane phospholipid content lowers the enzymatic activity of electron transport complexes. *Biochemistry* **53,** 5589–5591 CrossRef Medline

85. Shaikh, S. R., Locascio, D. S., Soni, S. P., Wassall, S. R., and Stillwell, W. (2009) Oleic- and docosahexaenoic acid-containing phosphatidylethanolamines differentially phase separate from sphingomyelin. *Biochim. Biophys. Acta* **1788,** 2421–2426 CrossRef Medline

86. Schmid, E. M., Richmond, D. L., and Fletcher, D. A. (2015) Reconstitution of proteins on electroformed giant unilamellar vesicles. *Methods Cell Biol.* **128,** 319–338 CrossRef Medline